Short title: Adaptive homeostasis to drought in Arabidopsis

Adaptive growth homeostasis in response to drought in Iberian Arabidopsis accessions

Ángel Ferrero-Serrano[1] & Sarah M. Assmann[1]

[1]Biology Department, Penn State University, 208 Mueller Laboratory, University Park, PA, 16802, USA

One-sentence summary: Information on phenotype, genotype, and transcript abundance is integrated to identify both plasticity and homeostasis genes and processes associated with local adaptation to drought stress in Arabidopsis accessions of the Iberian Peninsula.

Author contributions: S.M.A & A.F-S. conceived the project, research plans and experimental design. A.F-S. performed the experiments while S.M.A provided guidance throughout the experimental work. A.F-S. analyzed the data and prepared the figures; S.M.A provided supervision with data analysis and figure preparation. S.M.A & A.F-S wrote the manuscript. A.F-S agrees to serve as the author responsible for contact and ensuring communication and assistance with the reproducibility of the results of this study.

ABSTRACT

Plants respond to environmental fluctuations through plastic phenotypic shifts. Whether a plastic response upon environmental variability is adaptive or not has been subject to debate. Using a set of Iberian Arabidopsis accessions, we quantified an interplay between passive plastic reductions in leaf areas that we found typical of accessions from productive environments and homeostatic leaf areas responses to drought typified by accessions originating from unproductive environments. Results from Genome-Wide Association Studies (GWAS) and Transcriptome Wide Association Studies (TWAS) highlight the role of auxin-related processes and, in particular, the possible role of the *SMALL AUXIN UP RNA 26* (*SAUR26*) gene in the regulation of the observed plastic responses. Homeostatic responses in leaf area potential following drought were typical of accessions with lower leaf area potential under well-watered conditions. Transcripts that were negatively associated with leaf area potential and positively associated with homeostatic and positive leaf area plasticity following drought showed functional enrichment in ion transport processes. We hypothesized that the contrasting plastic and homeostatic responses in leaf area potential were associated with differential intrinsic water use efficiency (WUE_i). We confirmed this relationship in a metanalysis conducted using previously published $\delta^{13}C$ measurements. Our results highlight the adaptive role of homeostatic leaf area response to water depletion arising from increased WUE_i. The concerted utilization of Genome-Wide Association Studies (GWAS), Transcriptome Wide Association Studies (TWAS), and expression Genome-Wide Association Studies (eGWAS) allows integration of phenotype, genotype, and transcript abundance to identify both “plasticity genes” and “homeostasis genes” associated with drought stress responses.

INTRODUCTION

Earth is undergoing a climate change scenario resulting in extreme weather events that are increasingly frequent and variable (Easterling et al., 2000; Meehl and Tebaldi, 2004; Schär et al., 2004). These changing conditions are creating opportunities for some species to spread beyond their native ranges (Chen et al., 2011) while posing a challenge to species that are currently adapted to their local environment (Holt, 1990). As sessile organisms, plants must complete their life cycle in their local environment and consequently are experiencing changing climate conditions at an increasing rate and severity. A developmentally plastic response (West-Eberhard, 2003) is accepted as an appropriate response to environmental change during the lifetime of an individual plant. However, simply because a given trait is plastic does not mean that this plasticity is adaptive (Ghalambor et al., 2007). Active plasticity is anticipatory in response to predictable environmental cues. On the other hand, passive plasticity is not anticipatory but a consequence, often proportional, to a resource limitation. Active plastic phenotypic responses to environmental cues are thus more likely to be adaptive than passive plasticity that unavoidably arises from unpredictable resource limitation (Dorn et al., 2000; van Kleunen and Fischer, 2005; Forsman, 2015). However, the

division between passive and active plasticity is not straightforward. It not only depends on whether the environmental factor is a reliable cue such as daylength or an unpredictable resource such as water (precipitation) but also on the phenotype under consideration. For example, when plants are subjected to drought, their growth is limited, a passive response. Still, they can also respond actively by accelerating the onset of the reproductive stage (early flowering time).

The study of passive plastic responses to changes in resource availability can provide insights into plant responses to climate change-related events that are unpredictable. Water availability is indeed unpredictable, as the frequency and intensity of precipitation vary seasonally, annually, and geographically (Loik et al., 2004). Drought is thus among the strongest factors driving adaptation in plants (Siepielski et al., 2017; Exposito-Alonso et al., 2019). Climate projections for the remainder of the 21st century predict precipitation extremes to become more severe (Donat et al., 2016) and for this reason, understanding the genetic basis and adaptation potential of phenotypic traits and their plastic or homeostatic responses to drought is paramount.

Water availability ranges in a continuum from critically low to abundant and even excessive. The distribution of phenotypic traits and their plasticity in a population is often continuous (Galton, 1894) because they are influenced by variation in a large number of genes. The effect of many of these variants is additive or synergistic and of small effect individually (Fisher, 1919), and thus difficult to identify (Barton et al., 2019; Sohail et al., 2019). For example, leaf area displays natural intraspecific variation and varies in a continuous manner in response to resource availability. Leaf area is an important trait in relation to carbon and water fluxes: the degree of growth and leaf area production is indicative of the total amount of light intercepted by plants, assimilated carbon, but also evaporative water loss. Leaf area response to drought is not only of interest from an ecological perspective; for instance, biofuel production from non-grain biomass depends on vegetative growth (Varvel et al., 2008; Pols and Spahn, 2014).

The Iberian Peninsula is a drought-prone region particularly vulnerable to climate change effects on precipitation (Vicente-Serrano, 2006a; Vicente-Serrano, 2006b; Coll et al., 2016; Páscoa et al., 2017). The Iberian Arabidopsis population is particularly valuable because its accessions originate from a broad range of environments (Lobo et al., 2001; Rey Benayas and Scheiner, 2002). These accessions represent the region in continental Europe with the highest genetic diversity in Arabidopsis (Cao et al., 2011; The 1001 Genomes Consortium, 2016). The population structure of the Iberian accessions is well-defined (Picó et al., 2008; The 1001 Genomes Consortium, 2016), and previous studies in the Iberian population have provided considerable insight into the evolution and development of Arabidopsis (Picó et al., 2008; Montesinos et al., 2009; Gomaa et al., 2011; Méndez-Vigo et al., 2011; Montesinos-Navarro et al., 2011; Picó, 2012; Manzano-Piedras et al., 2014; Wolfe and Tonsor, 2014; Vidigal et al., 2016; Exposito-Alonso et al., 2018a; Marcer et al., 2018).

Natural populations of Arabidopsis, including those of the Iberian Peninsula, constitute an important component of the 1001 Genomes Project (The 1001 Genomes Consortium, 2016). The Arabidopsis 1001 Genomes Project provides high-quality full genome information for 1,135 inbred accessions collected from geolocated sites across an extensive distribution range, with a well-

studied population history (The 1001 Genomes Consortium, 2016; Durvasula et al., 2017), and well-characterized local environments (Ferrero-Serrano and Assmann, 2019). In addition, a reference panel is available with transcript abundance data for 727 Arabidopsis accessions (Kawakatsu et al., 2016), including 665 accessions that overlap with the collection of accessions included in the 1001 Genomes project (The 1001 Genomes Consortium, 2016); 189 of the 1,135 accessions are from the Iberian peninsula. This information provides the tools needed to study the genetic basis of phenotypic potential (i.e., the normalized maximum phenotypic value) and its plastic responses to a limiting resource such as drought.

In addition to GWAS, natural variation in abiotic stress-responsive transcript abundance can identify adaptive mechanisms (Des Marais et al., 2012; Lasky et al., 2014). Transcriptome Wide Association Studies (TWAS) associate transcript abundance with phenotypic traits (Gusev et al., 2016; Kremling et al., 2019), while eGWAS identifies candidate SNPs (expression SNPs or eSNPs) that control transcript abundance. Here, we utilize GWAS, TWAS, and eGWAS to identify the natural genetic and transcript abundance variation underlying both plastic and homeostatic responses to drought. We uncover an adaptive homeostatic growth strategy in accessions from less productive environments, dissect its genetic basis, and conclude that, just as has been argued previously for plasticity, homeostasis is under genetic control and of evolutionary importance.

RESULTS

Natural variation in leaf area and plasticity in response to long-term drought

To quantify phenotypic variation in Iberian Arabidopsis accessions exposed to sustained drought, we conducted a common garden experiment (Fig. 1A). We used image analysis to derive rosette leaf area for 43 Iberian accessions grown under well-watered or drought conditions (Fig. 1B, C; Table P1). As expected, we observed a reduction in leaf area resulting from drought in most genotypes, as evident from the phenotypic reaction norms, while a small number of accessions exhibited constant or increased leaf area under drought (Fig. 1A,D,E). Based on these data, we calculated leaf area potentials (Fig.1B,C,S,E) and plasticity indexes. We define leaf area potential as the normalized maximum phenotypic value realized by any given accession under each condition of the experiment (well-watered or drought). We used potential rather than actual values in order to allow comparison of relative leaf area of each accession within the study population between both watering regimes.

A leaf area plasticity index was calculated (Bouslama and Schapaugh, 1984) for each accession based on the difference in leaf area potential between drought and well-watered conditions, i.e., based on the reaction norms in Fig. 1F; Table P1. Genetic variants significantly associated with this parameter were identified by GWAS (Fig. 2A; Table G3). Gene ontology (GO) analysis of functions associated with the genes harboring the variants identified by GWAS revealed an enrichment in auxin-related functions (Fig. 2A; Table GO3). Among the variants identified from GWAS (Fig. 2A; Table G3) and TWAS (Table T1,T2) as associated with leaf area plasticity, we

highlight two co-varying SNPs in the 5' and 3' UTR of *SMALL AUXIN UP RNA 26* (*SAUR26***,** AT3G03850**)** (Figure 2B). We also found from eGWAS that the transcript levels of *SAUR26* are regulated by this genetic variation (cis-regulation; Fig. 2C; Table G6).

We illustrate the haplotypic differences in leaf area plasticity for *SAUR26* that we identify in our study (Figure 2B). Accessions harboring the minor *SAUR26* haplotype display negative plasticity in leaf area while the major haplotype is associated with homeostatic and positive plasticity responses in leaf area in response to drought (Fig. 2D; Wilcoxon *P*-value < 0.001). These haplotypic differences were also associated with the transcript levels of *SAUR26* (Figure 2C), which we confirmed both in the group of accessions included in our study (Wilcoxon *P*-value < 0.001) as well as in the 189 Iberian accessions included within the 1001 Genomes Project (Fig. 2E; Wilcoxon *P*-value < 0.001). Both the genetic variation defined by this haplotype in *SAUR26* and the resulting transcript abundance are associated with the interplay between plasticity and homeostasis that we define in our study (Fig. 2D,F). These results highlight *SAUR26* as a candidate regulator of leaf area plasticity in response to drought (Fig. 2G).

We conducted a GWA analysis of leaf area potential based on the genome-wide association of individual SNPs for leaf area in response to drought (Fig. S1A, Table G1, G2). In our GWA analysis on leaf area potential (Fig. S1A, Table G1, G2), no SNPs were found that were associated with leaf area potential under both well-watered and drought conditions, i.e., no SNPs that would be depicted as horizontal lines in Fig. S1A. The results from TWA analysis were strikingly different, identifying transcripts associated with both leaf area plasticity (Fig. S1B) and leaf area homeostasis (Fig. 3). A TWA analysis identified five transcripts that are positively correlated with leaf area potential under both well-watered and drought conditions: *SOFL2*, *CPN60B*, *AT5G02244*, *CKL8*, and *IBH1* (Fig. 3A). This means that accessions with higher transcript abundance of these genes display higher leaf area potential under both well-watered and drought conditions. We highlight *IBH1* as an example (Fig. 3B). Conversely, we identified four genes negatively correlated with leaf area potential such that accessions with a higher transcript abundance display lower leaf area potentials under both well-watered and drought conditions: *RHF1A*, *AT5G60160*, *AT4G15260*, and *AT5G16800* (Fig. 3A). We highlight *RHF1A* as an example (Fig. 3C).

Trade-off between growth, plasticity and intrinsic water use efficiency

We determined that the plastic leaf area responses we observed in our study were typical of accessions from more productive habitats, while homeostatic responses were typical of accessions from less productive habitats (Fig. S2). We next explored the relationship between leaf area potential in the absence of drought and its plastic response when drought is imposed. In Figure 4A, orange points depict accessions that display a reduction in leaf area in response to drought (negative plasticity) but that in the absence of drought display a high leaf area potential. Blue datapoints represent those accessions with homeostatic or positive growth responses to drought and low leaf area potential under well-watered conditions. Red points are accessions with negative plastic responses and low phenotypic potential. Finally, green datapoints are those accessions displaying

homeostatic or positive responses to drought that exhibit relatively high leaf areas in the absence of drought. We observe a trade-off between growth, indicated by high leaf area potential in the absence of drought, and leaf area homeostasis in response to drought. Accessions with higher leaf area potential displayed higher plastic reductions in leaf area potential when subjected to drought. On the contrary, accessions with lower leaf area potential under well-watered conditions display homeostatic phenotypic responses to drought (Fig. 4A).

We performed a GWA analysis (Fig. 4B; Table G1,G3) to determine the genetic basis of the trade-off between growth and homeostasis in response to drought illustrated in Fig. 4A. The green datapoints (representing four different genes) are those significantly associated with both leaf area potential and plasticity index and thus are candidate regulators of the trade-off. Among the candidate variants, we identified two co-varying SNPs in *PR5K-LIKE RECEPTOR KINASE* (*PR5K, AT5G38280*). The role of *PR5K* in drought and growth processes is not known, but another *PR5K-LIKE RECEPTOR*, *PR5K2,* is a key negative regulator of ABA signaling via phosphorylation of PP2C phosphatases such as *ABI1* and *ABI2* (Baek et al., 2019). We also identified two non-co-varying SNPs in *RAP2.7* as potential regulators of the trade-off between leaf area potential and plasticity. *RAP2.7* is part of the AP2 family of transcription factors, and we would expect it to be involved in flowering time processes (Du et al., 2020) rather than growth and plastic leaf area growth responses to drought. *WRKY DNA-binding protein 51* (*WRKY51***,** *AT5G64810*) has been previously linked to defense responses (Gao et al., 2011) but not to drought, leaf area, or plasticity. Finally, the function of *AT5G16990* has not been previously characterized. Gene Ontology analysis on the 17 genes that include the 50 SNPs with the strongest association with leaf area potential reveal an enrichment in responses to osmotic and salt stress (Table GO3). This will become relevant to the tradeoff between growth and plasticity as shown by our analysis of this process using TWAS, described below.

Figure 4C depicts the relationship between transcript abundance and the observed trade-off between growth and homeostasis in response to drought (Table T1,T2). Orange datapoints in Fig. 4C are transcripts with higher abundance in those accessions that are plastic and display higher leaf area potentials under well-watered conditions (depicted in orange in Fig. 4A). Conversely, blue points in Fig. 4C are transcripts with higher abundance in those accessions that are homeostatic and display lower leaf area potentials under well-watered conditions (depicted in blue in Fig. 4A). Gene Ontology analysis reveals that the transcripts negatively associated with leaf area potential are involved in ion transmembrane processes (Table GO3). This enrichment is also confirmed in the 30 transcripts depicted as blue datapoints in Fig. 4C (Table GO5).

A relationship between $\delta^{13}C$ and intrinsic water use efficiency has been confirmed in natural populations of Arabidopsis (Juenger et al., 2005; Easlon et al., 2014). Following this, we analyzed the $\delta^{13}C$ values recorded by Dittberner et al. (2018), available for 21 of the accessions used in our study. The results revealed a trade-off between plasticity and WUE_i (Fig. 4D). Accessions that exhibit strong negative plasticity in the presence of drought have a lower intrinsic water use efficiency in the absence of drought (more negative $\delta^{13}C$ values). Those accessions that maintain

leaf area in response to drought display a higher water use efficiency in the absence of drought (more positive $\delta^{13}C$ values).

We found no genetic variants associated with the observed trade-off between intrinsic water use efficiency and leaf area plasticity in response to drought (Fig. 4E; Table T1,T2), i.e., no datapoints in the upper right quadrant of Fig. 4E. However, TWA analysis (Table S2) provided insight into this trade-off. Red datapoints in Fig. 5F are transcripts with higher greater abundance in those plastic and less water-use efficient accessions depicted in red in Fig. 4D. Conversely, green points in Fig. 4F represent transcripts with greater abundance in the homeostatic and water-use efficient accessions depicted in green in Fig. 4D. GO analysis revealed an enrichment in snRNA and rRNA pseudouridine synthesis (Table GO7) for transcripts that display higher abundance in accessions with high negative plastic responses and lower WUE_i (red datapoints in 4F). We chose *CNGC16* and *AHA4* (see Discussion) to exemplify transcripts with opposed relationships to leaf area plasticity and water use efficiency (Fig. 5).

Intrinsic water use efficiency in the Iberian population

We determined that in our study, accessions that displayed positive growth or homeostasis in leaf area in response to drought (Fig 4A) also had higher WUE_i in the absence of drought (Fig. 4D). We then conducted a meta-analysis on the 95 Iberian accessions with $\delta^{13}C$ information from a previous study focused on the global Arabidopsis population (Dittberner et al., 2018). GWA analysis of these accessions rendered a distinctive peak in a single gene, identifying a haplotype consisting of eight co-varying SNPs in *ClpX3* (*AT1G33360*; Fig. 6A; Table G5), an ATP-dependent Clp protease. More informative was the TWA analysis of water use efficiency determined from ($\delta^{13}C$) values in the 88 Iberian accessions with both published transcript abundance and $\delta^{13}C$ information: we uncovered a distinctive enrichment in photosynthesis-related genes (Table. GO8) in transcripts that are upregulated in accessions with high water use efficiency (more positive $\delta^{13}C$ values; Fig. 6B; Fig. S4; Table T1,T2). We highlight the positive relationships uncovered for the transcript abundance of *RuBisCO small subunit 2B* (*AT5G38420*; *RBCS2B;* Fig. 6C), *PLASMA MEMBRANE INTRINSIC PROTEIN 1;5* (*AT4G23400*; *PIP1;5*; Fig. 6D) with WUE_i. Finally, we highlight the positive relationship between the transcript abundance of *SAUR26* and WUE_i (Fig. 6E), in concordance with the findings of our study.

DISCUSSION

Identifying candidate regulators of passive plasticity and adaptive homeostasis

There is an adaptive trade-off between growth and drought resistance in plants (Zhang et al., 2020). Plants adapted to more productive habitats with higher and more constant precipitation regimes favor decreased water use efficiency and increased carbon capture, producing increased leaf areas to compete for aboveground resources with neighbors (Tilman, 1988). Conversely, plants adapted

to unproductive environments typically fix less carbon, have higher water use efficiency, and display low growth rates, even when grown in rich environments (Parsons, 1968; Chapin, 1991), and are typical stress-tolerant (Billings and Mooney, 1968; Grime, 1977). In this study, we observe that accessions with higher leaf area potentials in the absence of drought display strong and negative plastic responses to drought (Fig. 1). On the other hand, accessions with lower leaf area potential in the absence of drought exhibit leaf area homeostasis or even positive leaf area potential plastic responses in response to drought (Fig. 1,4A).

Natural variation in the degree of plasticity among different ecotypes (accessions in the case of Arabidopsis) that are subjected to similar depletions in water availability can provide valuable information on the adaptive/neutral/maladaptive role of this plastic response. The variation in leaf area in Arabidopsis accessions in response to drought in this study can be grossly divided into passive and negative phenotypic plasticity in accessions adapted to richer environments (high Net Primary Productivity in spring, NPP spring), vs. adaptive phenotypic homeostasis responses observed in accessions originating from less productive areas of the Iberian Peninsula (low NPP spring) (Fig. S2). We sought to identify the genetic basis of these contrasting ecological strategies.

Identifying causal genetic variants related to an abiotic stress response such as drought is challenging given the polygenic nature of these responses (Exposito-Alonso et al., 2018b). Moreover, here, our main interest was not to identify natural variation associated with well-watered or drought phenotypes, but rather natural variation associated with the degree of plasticity evoked in response to drought, i.e., natural variation associated with reaction norms, rather than with phenotypes in one environment or the other (well-watered or drought). Reaction norms in leaf area in response to drought (Fig. 1E, F) illustrate the plasticity index that we calculated based on the difference in leaf area potential between drought and well-watered conditions (Table P1). In exploring the genetic basis of plasticity, we identified the 31 genes corresponding to the top 50 candidate SNPs with the highest strength of association with the leaf area plasticity index that we calculated (Figure 2B; Table G3). Of these 31 genes, 20 have been previously characterized, and many of these are related to auxin regulation and leaf expansion. This enrichment in auxin-related processes was confirmed by GO analysis (Table GO3). The variant with the strongest association with the plastic response to drought was the auxin efflux carrier family protein *PIN8* (*AT5G15100*). The SNPs with the third and fourth-highest scores (strength of association) correspond to co-varying variants in *AUXIN RESPONSE FACTOR 16* (*ARF16*; *AT4G30080)*. Among the candidates, we also obtained two co-varying SNPs in *SMALL AUXIN UP RNA 26* (*SAUR26*; *AT3G03850*); two variants in *AGAMOUS-like 15* (*AT5G13790*; *AGL15*), a gene that negatively regulates auxin signaling in Arabidopsis (Zheng et al., 2016); and three variants in *LONESOME HIGHWAY LIKE 1* (*LL2*; *AT2G31280*), an atypical basic helix-loop-helix (bHLH) transcription factor known to regulate early xylem development downstream of auxin (Ohashi-Ito et al., 2013). Among the candidates that are not included in the GO category “response to auxin”, we find four co-varying SNPs in the *Basic helix-loop-helix (bHLH) DNA-binding family protein MYC3* (AT5G46760), a known regulator of glucosinolate biosynthesis (Schweizer et al., 2013). Auxin negatively regulates glucosinolate levels, and this regulation appears to integrate growth and stomatal regulation during

drought (Salehin et al., 2019). TWAS analysis also revealed associations with auxin through glucosinolate biosynthesis: GO biological process analysis on positively correlated candidates resulting from TWAS analysis on leaf area plasticity index for drought revealed an enrichment of glucosinolate biosynthesis genes (Table S6).

We found that among the auxin-related variants associated with leaf area plasticity (Fig. 2A), SNPs in *SAUR26* were of particular interest. The majority of characterized *SAUR* genes are positive regulators of plant growth (Spartz et al., 2014; Li et al., 2015; Stortenbeker and Bemer, 2019). The two associated variants in *SAUR26* were found in the 5' and 3' UTR, respectively (Fig. 2B), regions of the ORF that typically regulate gene expression. Indeed, we found the transcript levels of *SAUR26* to be associated with the genetic variation in *SAUR26* itself (cis-regulation; Fig. 2C), which we confirmed both in the group of accessions included in this study and in the 189 Iberian accessions included within the 1001 Genomes Project (Fig. 4E). The minor haplotype is associated with negative plasticity in leaf area in response to drought. Conversely, the major haplotype, associated with higher transcript abundance of *SAUR26*, is associated with leaf area homeostasis and positive plastic responses (Fig. 2D).

Relevant to the non-discrete distribution of the plastic responses in the accessions that we studied, variation in transcript abundance of *SAUR26* explained 17% of the observed plastic response in leaf area to drought in our study (Figure 2F, G). The importance of *SAUR26* is supported by previous work that revealed natural genetic variation in *SAUR26* associated with growth thermo responsiveness of the rosette compactness index (Wang et al., 2019) and cis elements in the 5' upstream region or the 3'UTR region of *SAUR26* that were responsible for this response (Wang et al. 2021). This conclusion is also supported by our meta-analysis of the larger Iberian population with transcriptome data, which also identified *SAUR26* transcript abundance as positively correlated with higher water use efficiency (Fig. 6B,C) along with other related auxin-related transcripts such as *AUXIN RESISTANT 3* (*AXR3*, also known as *IAA17*, *AT1G04250*) (Leyser et al., 1996) and *SMALL AUXIN UPREGULATED 15* (*SAUR15*, *AT4G38850*) (Oh et al., 2014) (Fig. 6B). As we uncover in this study, both transcript abundance and natural genetic variation in *SAUR26* cis-regulatory elements are associated with the interplay between plasticity and homeostasis in leaf area potential following drought stress (Fig. 2, Table G3,T1,T2). Interestingly, the minor haplotype frequency for this haplotypic variant in our study sample (Minor haplotypic frequency, MHF = 38.09%) has a frequency similar to the frequencies we find in the 189 accessions within the Iberian population (MHF = 35.98). However, the minor haplotype in the Iberian population becomes the haplotype in higher frequency (64.14%) in the global 1001 Genomes collection. We know that Iberian Arabidopsis populations locally adapted to drought conditions in this region out-perform accessions from wetter areas of Northern Europe when both are exposed to drought (Exposito-Alonso et al., 2019). Following this, given that the major haplotype in our study is associated with homeostatic responses to drought (Fig. 2D), and that its frequency became less frequent outside the drought-prone Iberian region, we can speculate that this *SAUR26* haplotypic variant is under selection in the Iberian population conferring an adaptive advantage to water-limited conditions in the region.

The study of the strength of association of genetic variation with leaf area plasticity provides us with candidates that reveal a binary answer: one allele is associated with plastic reductions in leaf area while the alternative allele will display an association with either homeostatic or positive plasticity (increase in leaf area potential) under drought. We did not identify any SNPs associated with leaf area potential under both well-watered and drought conditions. Therefore, we could not define the genetic basis of growth homeostasis under drought using GWAS (Fig. S1). On the other hand, reaction norms based on the strength of association of transcript abundance with leaf area potential identify five transcripts that are positively correlated with leaf area potential under both well-watered and drought conditions (Fig. 3A). This means that accessions with higher transcript abundance for those genes display higher leaf area potential under both well-watered and drought conditions. Conversely, we identified four transcripts negatively correlated with leaf area potential such that accessions with a higher transcript abundance of those genes display lower leaf area potentials under both well-watered and drought conditions. Therefore, these nine genes are strong functional candidates for homeostatic regulation of leaf area potential.

Most of the candidate genes we obtained from this analysis have not been characterized, and for those that have, their function is not necessarily known to be involved in growth processes leading to differential leaf area. Among the homeostatic transcripts positively correlated with leaf area potential, *ILI1 binding bHLH 1* (*IBH1*, AT2G43060) (Fig. 3B) has been previously shown to improve drought tolerance in Arabidopsis (Moreno et al., 2018) which is consistent with the homeostatic response that we observe. At the same time, ectopically expressed *IBH1* represses cell elongation in Arabidopsis (Ikeda et al., 2012; Zhiponova et al., 2014), and expression of Arabidopsis *IBH1* in transgenic tobacco plants (*Nicotiana tabacum*) induces a dwarf phenotype (Nagatoshi et al., 2016). In our study, we observe a direct relationship between the natural variation in the transcript abundance of *IBH1* and leaf area potential, which seems counterintuitive based on these latter reports, perhaps reflecting an interaction between genotypic background and *IBH1*. *SOFL2* (Fig. 3C), another candidate positively correlated with leaf area potential and homeostasis. has been previously reported to confer an increase in the levels of specific cytokinins, which positively regulate plant growth (Zhang et al., 2009). From inspection of the four candidate homeostatic transcripts that are negatively correlated with leaf area potential, only *RING-H2 GROUP F1A* (*RHF1A*; *AT4G14220*) has been previously characterized. While the role of *RHF1A* in the regulation of leaf growth has not been studied, it directly interacts with *KIP-related protein 6* (*KRP6*; *AT3G19150*) (Liu et al., 2008). The overexpression of *KRP* genes reduces cell proliferation by inhibiting CDKs, resulting in small plants with large cells (De Veylder et al., 2001). We can hypothesize that higher transcript abundance of *RHF1A* may result in reduced vegetative growth by interacting with *KRP* genes.

To increase leaf area potential and sacrifice WUE_i or increase WUE_i and sacrifice leaf area potential?

We found that accessions with higher leaf area potential displayed greater plastic reductions in leaf area potential (negative leaf area plasticity index) when subjected to drought (Fig. 4A). This response is presumably neither adaptive nor maladaptive but a consequence or passive response to a limited resource rather than an active response. Consistent with this, accessions with plastic responses are typical of productive habitats, while the homeostatic responses that we observed in our study typify accessions collected from less productive habitats (Fig. S2).

Gene Ontology analysis on the 17 genes that include the 50 SNPs with the strongest association with leaf area potential (green and yellow datapoints in Fig. 4B) reveals an enrichment in responses to osmotic and salt stress (Table GO1). Gene Ontology analysis also reveals that the transcripts negatively associated with leaf area potential are involved in ion transmembrane processes (Table GO2). This enrichment is also confirmed in the 30 transcripts depicted as blue datapoints in Fig. 4C (Table GO5). We hypothesized that these processes are related to the greater water use efficiency of accessions with reduced growth rates typical of unproductive environments. Indeed, plant species with low relative growth rates are known to exhibit high intrinsic water use efficiency (WUE_i) (Angert et al., 2009; Kimball et al., 2012). WUE_i is defined as the ratio between instantaneous carbon gain and transpirational water loss, typically calculated per unit of leaf area (Condon et al., 2002). In support of our hypothesis, the homeostatic response in leaf area potential in response to prolonged drought that we observe in our study correlates positively with a high predicted water use efficiency recorded by Dittberner et al. (2018) for the same accessions (Fig. 4D). While we regard the observed plasticity in response to drought as a passive response to resource availability, we propose that the observed leaf area homeostasis is an adaptive response.

These observations are consistent with what has been described before in classic ecological studies, as well as in studies on crop cultivars (Kasuga et al., 1999; Ferrero-Serrano and Assmann, 2016; Ferrero-Serrano et al., 2018). There were no overlapping SNPs associated with both the leaf area plasticity index and WUE_i (Fig. 4E). However, when we compare the candidates obtained from TWAS analysis, we identify transcripts associated with both low WUE_i and a negative plastic response in leaf area when subjected to sustained drought. Conversely, we identify a set of transcripts that is significantly associated with both leaf area homeostasis (more positive leaf area plasticity index) and increased WUE_i (Fig. 4F). To exemplify these opposed responses to drought, given the enrichment in ion transport genes that we found in the transcripts regulating the tradeoff between leaf area plasticity and potential (Fig. 4C; Table GO5), we highlight two of the genes identified by TWAS, with opposite correlations between transcript abundance and relative leaf area plasticity (Fig. 6A,B vs. Fig. 6C,D): *CYCLIC NUCLEOTIDE GATED CHANNEL 16* (*CNGC16*; *AT3G48010*) and Plasma Membrane H^+ ATPase 4 (*AHA4*; *AT3G47950*).

CNGCs are a superfamily of cation channels permeable to divalent and monovalent cations, including Ca^{2+} and K^+ (Köhler et al., 1999; DeFalco et al., 2016). *CNGC*s like *CNGC5* and *CNGC6* have been previously reported to be required for a cyclic GMP (cGMP)-activated nonselective Ca^{2+}-permeable cation channel activity in the plasma membrane of Arabidopsis guard cells (Wang et al., 2013) associated with stomatal closure. In particular, *CNGC16* is critical for reproductive success following drought stress (Tunc-Ozdemir et al., 2013). Consistent with these functional

435 roles, in our study, higher transcript abundance of *CNGC16* is found in accessions with positive leaf
436 area plasticity indexes under drought (leaf area homeostasis; Fig. 5A); and with high WUE_i (Fig.
437 5B).
438 The inverse relationship is found for the transcript abundance of *AHA4*. Auxin-mediated
439 signaling and growth involve the activation of plasma membrane H^+ ATPases (Hager, 2003;
440 Rober-Kleber et al., 2003; Takahashi et al., 2012), and activation of H^+ ATPases also drive stomatal
441 opening, which results in decreased WUE_i. This is supported by the negative correlation between
442 leaf plasticity and *AHA4* transcript abundance that we observe, wherein accessions with higher
443 transcript abundance of *AHA4* display strong negative plastic responses in leaf area potential in
444 response to drought (Fig. 5C). Accordingly, the increased transcript abundance of *AHA4* is also
445 associated with reduced WUE_i (Fig. 5D).
446 We have described two opposed processes in response to sustained drought. On the one
447 hand, accessions displaying higher leaf area potential in the absence of drought display a higher
448 plastic reduction in leaf area potential following drought than accessions with lower leaf area
449 potential in the absence of drought. Indeed, species with high relative growth rates are known to
450 exhibit low WUE_i (Angert et al., 2009; Kimball et al., 2012). We argue that accessions from less
451 productive environments in the Iberian Arabidopsis population are adapted to drought and maintain
452 homeostatic response in leaf area to drought through their increased intrinsic water use efficiency.
453 Given the increased plastic responses in leaf area that we found in accessions with lower
454 water use efficiency, we next conducted a meta-analysis on the larger set of 95 Iberian accessions
455 with $\delta^{13}C$ information from a previous study focused on the global Arabidopsis population
456 (Dittberner et al., 2018). Upon inspection of the candidates obtained from GWAS analysis of $\delta^{13}C$
457 values in Iberian accessions, we could not identify an overarching functional theme, neither from
458 GO biological process analysis nor from published studies of the genes in which the associated
459 variants were located. However, we obtained a distinctive peak consisting of eight co-varying SNPs
460 in a single gene, *ClpX3* (*AT1G33360*; Fig. 6A), an ATP-dependent Clp protease. The Clp protease
461 system is a central component of the plastid protease network, ensuring the removal of aggregated
462 and misfolded proteins (Nishimura and van Wijk, 2015). *Clp* core mutants *clpr2* and *clpr4* null
463 mutants display a remarkable loss of chlorophyll (95 to 98% reduction) and photosynthetic
464 capacity, turning entirely white when grown under high light (Kim et al., 2009). The *clpr4-1* mutant
465 displays a downregulation of photosynthetic thylakoid proteins, the cytb_6f complex, the ATP-
466 synthase, and the NDH complex, as well as stromal *RuBisCO* large and small subunits, and allene
467 oxide synthase (Kim et al., 2009).
468 We conducted TWAS analysis of WUE_i determined from $\delta^{13}C$ values in the 88 Iberian
469 accessions with both $\delta^{13}C$ information (Dittberner et al., 2018) and published transcript abundance
470 (Kawakatsu et al., 2016). Gene Ontology (GO) biological process analysis on the resultant 45
471 candidates positively correlated with $\delta^{13}C$ uncovered an unequivocal enrichment in photosynthesis-
472 related genes for transcripts that are upregulated in accessions with high WUE_i (more positive $\delta^{13}C$
473 values; Fig. 6B, S3; Table GO8). During photosynthesis, plants discriminate against $^{13}CO_2$ in the
474 reaction center of *Ribulose 1, 5-biphosphate carboxylase/oxidase* (*RuBisCO*). As stomata close to

minimize water loss in response to drought, the discrimination against ^{13}C is less intense because the internal CO_2 concentration (C_i) becomes unavoidably reduced, reflecting a trade-off between carbon gain and water loss. As a result of their reduced C_i, water-efficient plants experience lower CO_2 concentrations at the sites of carboxylation (C_c) and have more positive $\delta^{13}C$ values. Among the candidates from our TWAS analysis that are positively related to water use efficiency, we found *RuBisCO small subunit 2B* (*AT5G38420*; *RBCS2B;* Figs. 6B, D). An upregulation in *RuBisCO* may compensate for suboptimal CO_2 concentrations at the sites of carboxylation that plants from drought-prone environments typically experience. Among these candidates, we also find *Sedoheptulose-bisphosphatase* (*SBPASE*, *AT3G55800*), a key enzyme in the Calvin Cycle (Lefebvre et al., 2005) and *MATURATION OF RBCL 1* (*MRL1*, *AT4G34830*), a post-transcriptional regulator of *RuBisCO large chain* (*RBCL*, *ATCG00490*) mRNA (Johnson et al., 2010).

Also among the candidates we obtained from this analysis is a member of the plasma membrane intrinsic protein (PIP) subfamily of aquaporins, *PLASMA MEMBRANE INTRINSIC PROTEIN 1;5* (*AT4G23400*; *PIP1;5*; Figs. 6B,E). While the functional role of *PIP1;5* in these specific processes has not been characterized, PIPs are known to regulate water flux in guard cells as well as membrane permeability to CO_2 in the mesophyll, with an important effect on mesophyll conductance and CO_2 concentration at the sites of carboxylation (C_c) (Groszmann et al., 2017). Thus, PIP1;5 is also a candidate regulator of photosynthetic rates. Also, among the candidates are *NADH dehydrogenase-like complex M* (*NdhM*, *AT4G37925*), required for *NdH* complex assembly (Ifuku et al., 2011), and *High cyclic electron flow 1* (*HCEF1*; *AT3G54050*) (Livingston et al., 2010), both regulators of cyclic electron flow around PSI (Yamori et al., 2011), *ATP-Synthase δ-Subunit* (*ATPD*, *AT4G09650*) (Maiwald et al., 2003), *Photosystem I reaction center subunit PSI-N* (*PSAN*, *AT5G64040*) (Haldrup et al., 1999), *Photosystem II subunit O-2* (*PSBO2*; *AT3G50820*) (Murakami et al., 2005).

Among the candidates that are negatively related to WUE_i, we find the transcripts of nine genes, of which only two are characterized: *YELLOW STRIPE like 8* (*YSL8*, *AT1G48370*) (Waters et al., 2006) and *PIGMENT DEFECTIVE EMBRYO 135* (*PDE135*, *AT2G26510*) (Niopek-Witz et al., 2014). We can speculate that the large proportion of uncharacterized genes negatively associated with WUE_i may be the result of an increased lethality in the loss of function mutations in these genes. (Table GO9). We can further speculate that this enrichment reflects the transport of carbohydrates produced during photosynthesis to promote plant growth. This would be concordant with the tradeoff between growth and WUE_i that we observe in our study.

Limitations

Our study has revealed genetic variants associated with both plasticity and homeostasis in leaf area following drought. One limitation of our study is that while the number of accessions that we utilized would have been considered ample just a few years ago, with the more recent advent of GWA studies in Arabidopsis such studies typically include more accessions. If the number of accessions utilized is low, low-frequency variants may not be present in the subset of accessions

studied. This is less of a concern when we focus on variants that are undergoing selection and thus are at higher frequency in the population. Accordingly, in this study, we did not consider variants in frequencies lower than 10% as we were interested in adaptive genetic variation. In addition, we performed TWAS, which is less susceptible to this concern because it evaluates continuous variation in transcript abundance rather than the presence/absence of SNPs within the study population. Indeed, RNA-seq experiments often are conducted on very few genotypes, frequently comparing transcript abundance between just two genotypes: wild-type and a specific mutant of interest. Another limitation typical of GWAS is the fact that synthetic associations, non-causative markers that are within linkage disequilibrium with causative makers, are difficult to discern from true causative markers (Korte and Farlow, 2013; Sasaki et al., 2021). Identification of polygenic association signals through GWAS is also sensitive to bias introduced by uncorrected population structure that can also introduce a number of false positives in the resulting list of candidates (Barton et al., 2019; Sohail et al., 2019). There are statistical methods to address these issues, but such methods also introduce a number of false negatives due to over-correction (Korte and Farlow, 2013). Not correcting for confounding effects of population stratification, family structure, and cryptic relatedness can be minimized by focusing on regional collections, such as the Iberian population in this case, in which the challenges imposed by population structure are reduced (Frachon et al., 2018; Tabas-Madrid et al., 2018).

TWAS analysis does not suffer from the limitations imposed by false non-causal synthetic associations due to linkage disequilibrium and by population structure.(Korte and Farlow 2013; Joehanes et al. 2017). However, TWAS analysis also presents a series of challenges, as this method is sensitive to time and tissue-dependent expression (Li et al. 2020; Wainberg et al. 2019). The combined analysis of reference genomic (The 1001 Genomes Consortium 2016) and transcriptomic data (Kawakatsu et al. 2016), as done here, can partially ameliorate the limitations of each method.

The validation of candidates from both GWA and TWA studies also suffers from the challenge of restricted genetic backgrounds. Most often, the characterization of knock-out mutants of candidate genes is performed in a single genetic background, typically Col-0. Here, we instead validated our results by meta-analysis of the larger Iberian population. TWAS in this larger sample identified 31 out of the 45 candidate genes that we previously identified in the subset of 20 Iberian accessions in our study for which published $\delta^{13}C$ data were available (Table T1). Moreover, there are significant correlations between the results from our sample and the larger sample from both GWAS and TWAS (Fig. S4).

Conclusion

In our study, we find a gradient ranging from higher plasticity in response to resource limitation (drought) for generalist accessions originating from productive environments to increased specialization and decreased phenotypic plasticity in accessions originating from more marginal environments. The “passive” plasticity observed here may nevertheless be important over evolutionary time as it gradually allow adaptiveness in unproductive environments as the induced

change in resource availability moves the mean phenotype closer to the environment-specific optimum favored by selection (Waddington, 1953; Richards et al., 2006).

The adaptive role of plasticity has been at the center of a long-standing debate. Much work and discussion have been focused on the principle that if indeed plasticity is adaptive, it may be under genetic control (Bradshaw, 1965; Via et al., 1995); however, few relevant genes have been identified. Here we propose that not only plasticity but also homeostasis is under genetic control and important from an evolutionary standpoint. Moreover, we dissect the genetic basis of both plasticity and homeostasis in leaf area, identifying specific genes and regulatory variants implicated in each process. Our integrated application of GWAS, TWAS, and eGWAS identifies both candidate "plasticity variants" and candidate "homeostasis variants" that can be further studied.

Knowledge from natural populations of how plants adapt to their environment also can be incorporated in breeding and biotechnological approaches to crop improvement. We show here how the integrated application of GWAS, TWAS, and eGWAS yields insights into the genetic basis of responses to resource availability in Arabidopsis. A similarly integrative approach has identified water use efficiency traits in sorghum (Ferguson et al., 2020). Results arising from diverse genome-wide analyses in both model and crop species (Schindele et al., 2020) can now be used to inform powerful new CRISPR-based approaches for gene editing and modulation of transcript abundance toward crop improvement (Abudayyeh et al., 2017).

MATERIALS AND METHODS

Plant materials and phenotyping

Seeds for 43 Iberian accessions (Fig. 1A and Table S1 for the list of accessions) and Col-0, which we used as an internal reference, were cold-stratified for four days at 4°C to synchronize germination. Plants were grown in 10 cm square pots containing Metro-mix 360 potting mixture (Sun Gro Horticulture Canada Ltd) in a greenhouse with an average 500 μmol $m^{-2}s^{-1}$ photosynthetic photon flux density (PPFD) and temperatures of 22 °C during the day and 20°C during the night.

Stratified seeds were sown in soil in the Penn State University Biology Greenhouse. We imposed short day supplementary illumination (8h light: 16 h dark, with light supplied as natural daylight supplemented with 1000W metal halide lamps). For each accession, we grew one plant per pot, with five repetitions for each of control and drought treatments (10 plants for each individual accession), for a total of 440 plants (44 accessions x five control x five droughted plants). Both control and drought treatment were well-watered for the first 28 days, by maintaining the soil relative water content over 75%, as measured by monitoring pot weight daily and adding water when necessary. After 28 days, plants within the drought treatment were watered to soil saturation once every 10 days, while the well-watered treatment was maintained near field capacity throughout the duration of the experiment. The experiment continued for the entirety of the life cycle of the plants. Plants were randomized within the greenhouse on a weekly basis throughout the

experiment. At the end of the experiment 170 days later, nine accessions within the drought treatment that encountered mortality rates higher than 40% (two of the five replicates; Table S1) were excluded from downstream analysis

Photographs of rosettes were taken at the time of flowering and subsequently analyzed using ImageJ (http://imagej.nih.gov/ij/) to determine projected leaf area. For the associations between the phenotypic variables we obtained in this study, and the local environment, we inspected the data using Cook's distance (Cook, 1984; Altman and Krzywinski, 2016) to evaluate the influence of each datapoint on the fit. We considered values greater than 4/n to be overly influential. Based on this, we decided to retain outliers in our analysis except for the phenotypic values we obtained for the accession IP-Coc1 (accession id = 9535), which were consistently unrealistically influential across different phenotypes based on their extreme Cook's distance. We include these removed values in Table S1.

Determination of phenotypic potential and plasticity

Leaf area potential (LAP) is defined here as the normalized maximum leaf area (LA) value realized by any given accession under the conditions of these experiments. This index was calculated as $LAP = LA_i/LA_m$, where LA_i = leaf area produced by any individual accession and LA_m = average value for all accessions grown under the same conditions. Accordingly, leaf area potential (LAP) reflects the leaf area that any given accession displays in the absence of drought stress, divided by the average leaf area of the population in the absence of drought stress. A high leaf area potential reflects a higher vegetative growth of any given accession relative to the set of accessions utilized in this study. We used potential rather than actual values in order to compare the relative leaf area of each accession within the study population between both watering regimes.

Leaf area plasticity indexes were calculated based on an established definition (Bouslama and Schapaugh, 1984). Leaf area plasticity indexes to drought ($LAPI_d$) were calculated as: $LAPI_d = LAP_d - LAP_{ww}$; where LAP_d= leaf area potential under drought and LAP_{ww} = leaf area potential under well-watered conditions. Positive indexes reflect an increment in leaf area potential value for any given accession after drought treatment, not necessarily an increment in leaf area. For instance, a positive leaf area plasticity index does not necessarily imply leaf areas were higher under drought, but that under drought, a given accession displays a higher leaf area potential relative to the rest of accessions utilized in this study.

Reaction norms based on leaf area potential were employed to reflect plastic changes in phenotypic potential between the two treatments (well-watered vs. drought). The difference in leaf area potential between drought and well-watered conditions for the reaction norm of each accession is its leaf area plasticity index.

Genome-wide association study

We used a GWAS approach to identify polymorphisms associated with variation in phenotypic potential and plasticity. The online tool GWAPP (http://gwas.gmi.oeaw.ac.at/) was employed using a linear regression model (Seren et al., 2012). While the linear regression model does not address confounding effects of population stratification, family structure and cryptic relatedness (Price et al., 2010), it was employed here because those issues were minimized by our choice of a regional (Iberian) population (Frachon et al., 2018; Tabas-Madrid et al., 2018; Frachon et al., 2019).

We filtered out low frequency variants (MAF < 10%), to focus on variants less likely to be undergoing negative selection or to be spurious SNPs from sequencing errors. We obtained gene model annotation from the TAIR11 genome release. We defined the 'consensus' transcript variant as the variant producing the longest transcript. We predicted the effect of every SNP using SnpEff (Cingolani et al., 2012)(Table G1-G6).

Using the results from GWAS obtained from the association with leaf area potential, we obtained reaction norms that reflect plastic and homeostatic patterns of genome-wide associations of these traits in response to drought. For instance, genetic association plasticity indexes to drought (G_d) were calculated as: $GPI_d = G_d - G_{ww;}$ where G_d = Genome-wide association score (-log p-value) with any given phenotype under drought, and G_{ww} = Genome-wide association potential under well-watered conditions. The association between a phenotype and a SNP was considered more plastic as the genome-wide association score difference in the correlation coefficient between the two conditions reflected in the reaction norm (well-watered vs. drought) became greater. On the contrary, the association between a phenotype and any given SNP was considered to be homeostatic if found significantly associated to that trait under both conditions (well-watered and drought).

Transcriptome-wide association

We retrieved the transcriptome data generated by the Illumina HiSeq 2500 platform from rosette leaves of 727 Arabidopsis accessions (without biological replicates) from the GEO dataset with accession number GSE80744 and SRA study SRP074107 (Kawakatsu et al., 2016) and subsetted the 35 Iberian accessions that overlapped with the 43 Iberian accessions used in our study. Data wrangling was conducted using the dplyr (Wickham et al., 2015) and tidyr (Wickham and Henry, 2018) packages. Spearman's rank correlation coefficient between individual phenotypic values and individual transcript abundance values was calculated using the correlation function of the Hmisc package (Harrell Jr and Dupont, 2019). The stronger the association of the two variables, the closer the Pearson correlation coefficient, r, will be to either +1 or -1. We imposed a threshold based on this correlation coefficient ($0.4 \geq |r| \leq 4.0$). We considered this threshold to be appropriate after inspection of the results; it is a stringent value in relation to what has been used in previous TWAS studies in this species ($0.3 \geq |r| \leq 3.0$) (Lan et al., 2021).

Using the results from TWAS obtained from the transcript abundance association with phenotypic potential traits, we derived reaction norms to reflect plastic and homeostatic patterns of transcriptome wide associations of these traits in response to drought. For instance, transcriptome association plasticity indexes to drought ($Tr_{drought}$) were calculated as: $TrPI_{drought} = Tr_{drought} - Tr_{well-}$

$_{\text{watered;}}$ where $Tr_{drought}$ = transcriptome correlation coefficient potential with any given phenotype under drought, and $Tr_{well\text{-}watered}$ = transcriptome correlation coefficient under well-watered conditions. The association between a phenotype and any given transcript was considered to be homeostatic if found significantly associated with that trait (either positively or negatively) under both conditions (well-watered vs. drought). To focus on highly plastic transcriptome-wide associations, we isolated association between a phenotype and transcript that met the imposed a threshold based on its correlation coefficient ($0.4 \geq |r| \leq 4.0$) under one condition (well-watered or drought), but with a reaction norm that crossed the lack of correlation value ($r = 0$).

eGWAS

eGWAS was conducted by compiling the transcript abundance values of any given gene and extracting transcript abundance for that particular gene in the 727 Arabidopsis accessions from the GEO dataset with accession number GSE80744 and SRA study SRP074107 (Kawakatsu et al., 2016), then subsetting the 665 accessions included in the 1001 Genomes project (The 1001 Genomes Consortium, 2016). Regulatory variants are either cis or trans acting, depending on the physical distance between the genetic variant. cis-eSNPs were defined as those located within the ORF or the promoter region, which was defined as 5 kb upstream of the most distal transcription start site of the gene. Trans-eSNPs were defined as those located within the ORF/promoter region of a gene different from the one that is transcriptionally regulated by that genetic variant.

Meta-analysis of Iberian Arabidopsis accessions

To explore the local environment of this population, we retrieved 204 environmental parameters for these 188 Iberian accessions from AraCLIM (https://github.com/CLIMtools/AraCLIM) (Table SXX1). AraCLIM is a database that describes the local environment of the Arabidopsis accessions sequenced as part of the 1001 Genomes Project (Ferrero-Serrano and Assmann, 2019). We obtained from AraCLIM the moderate-resolution imaging spectroradiometer data corresponding to the spring months during the 2001-2010 period, to assess the Net Primary Productivity in the local environment of the accessions included in our study. (MOD17A2; Net Primary Productivity in the spring season) (Heinsch et al., 2003; Running and Zhao, 2015)

To integrate the information from previously published studies that included accessions from the Iberian Arabidopsis population, we retrieved available data on natural variation in intrinsic water use efficiency (WUEi, $\delta^{13}C$) previously recorded by Dittberner et al. (2018) from PhenoCLIM (https://github.com/CLIMtools/PhenoCLIM)(Table P1,P2)(Ferrero-Serrano and Assmann, 2019).

Analyses

All statistical analyses and figures were produced using R (Team, 2013). The code and data to easily reproduce the analysis, figures and tables in this manuscript are available at https://github.com/AssmannLab and Zenodo. Gene Ontology (GO) biological process analysis was performed using the open-source software ShinyGO v0.61: http://bioinformatics.sdstate.edu/go60/ (Ge et al., 2020) with the following settings: the search species was "*Arabidopsis thaliana*," the *P*-value cutoff (FDR) was 0.05, and the number of most significant terms to show was 10. To replicate these results, the lists of genes that were input into these analyses based on significance thresholds can be selected from Table G1-G6, T1,T2.

Supplemental data

The following supplemental materials are available

Figure S1. Genotypic and transcriptomic reaction norms based the strength of association of individual SNPs and transcripts highlights the variation of these associations depending on water availability.

Figure S2. Accessions from more productive areas display stronger negative plastic reductions in leaf area relative to accessions from less productive environments

Figure S3. Illustration of the photosynthesis-related transcript variants that regulate water use efficiency in Iberian Arabidopsis accession**.**

Figure S4. The accessions included in this study are representative of the Iberian accessions included in the 1001 Genomes project.

Table P1. Leaf area measurements recorded in this experiment (well-watered & drought). Calculated leaf area potential and plasticity, water use efficiency (WUE_i, $\delta^{13}C$) values recorded by Dittberner et al. (2018) and MOD17A2 net primary productivity) information obtained from AraCLIM (Ferrero-Serrano & Assmann, 2019) for the accessions included in our study.

Table P2. Water use efficiency (WUEi, $\delta^{13}C$) values recorded by Dittberner et al. (2018) for 95 Iberian Arabidopsis accessions.

Table G1. Candidates obtained from GWAS on leaf area potential under well-watered conditions. Only associations with a score ≥ 4 are included here. For a pre-filtered, as well as a full filtered version of this file, please visit the data repository.

Table G2. Candidates obtained from GWAS on leaf area potential under drought. Only associations with a score ≥ 4 are included here. For a full pre-annotated and filtered, as well as a full annotated and filtered version of this file, please visit the data repository. For a pre-filtered, as well as a full filtered version of this file, please visit the data repository.

Table G3. Candidates obtained from GWAS on leaf area plasticity. Only associations with a score ≥ 4 are included here. For a pre-filtered, as well as a full filtered version of this file, please visit the data repository.

Table G4. Candidates obtained from GWAS on water use efficiency (WUEi, δ13C) values recorded by Dittberner et al. (2018) for the accessions included in our study. Only associations

with a score ≥ 4 are included here. For a pre-filtered, as well as a full filtered version of this file, please visit the data repository.

Table G5. Candidates obtained from GWAS on water use efficiency (WUEi, δ13C) values recorded by Dittberner et al. (2018) for 95 Iberian Arabidopsis accessions. For a pre-filtered, as well as a full filtered version of this file, please visit the data repository.

Table G6. Candidates obtained from eGWAS on the natural variation in transcript abundance of SAUR26 extracted from Kawakatsu et al. (2016). For a pre-filtered, as well as a full filtered version of this file, please visit the data repository.

Table T1. Results from TWAS (r_s).

Table T2. Results from TWAS (*P*-value).

Table GO1. GO analysis on the 17 genes corresponding to the top 50 candidate SNPs resulting from GWAS analysis on leaf area potential under well-watered conditions.

Table GO2. GO analysis on negatively correlated candidates resulting from TWAS analysis on leaf area potential under well-watered conditions.

Table GO3. GO analysis on the 30 genes corresponding to the top 50 candidate SNPs resulting from GWAS analysis on leaf area plasticity index for drought.

Table GO4. GO analysis on the positively correlated candidates resulting from TWAS analysis on leaf area plasticity index for drought.

Table GO5. GO analysis on the negatively correlated candidates resulting from TWAS analysis on leaf area plasticity index for drought.

Table GO5. GO analysis on the transcripts with abundances that overlap negatively with leaf area potential under well-watered conditions, and positively with leaf area plasticity index for drought (blue datapoints in Fig. 4C).

Table GO6. GO analysis on the transcripts with abundances that overlap negatively with leaf area potential under well-watered conditions, and positively with leaf area plasticity index for drought (orange datapoints in Fig. 4C).

Table GO7. GO analysis on the transcripts with abundances that overlap negatively with leaf area plasticity index for drought and WUEi (red datapoints in Fig. 4F).

Table GO8. GO analysis on the positively correlated candidates resulting from TWA analysis of water use efficiency determined from (δ13C) values in 88 Iberian Arabidopsis accessions (Fig. 6A).

Table GO9. GO analysis on the negatively correlated candidates resulting from TWA analysis of water use efficiency determined from (δ13C) values in 88 Iberian Arabidopsis accessions (Fig. 6A).

Figures

Figure 1. Rosette leaf area observations at the time of flowering used to calculate leaf area potential and plasticity in this study (Table S1). A. Detail of the common garden experiment, illustrating the randomization of well-watered and drought treatments, as reflected in soil

coloration. **B.** Leaf areas for accessions grown under optimal conditions. **C**. Leaf areas for accessions under drought conditions. Accessions are arranged alphabetically. Bars represent means ±SE. **D.** Images illustrating the plastic and homeostatic responses to drought found among the accessions included in this study. **E.** Phenotypic reaction norms illustrating an overall reduction of leaf area in response to drought (t-test; *P*-value < 0.001). Violin distributions represent probability densities of leaf area (cm^2) among the accessions included in this study. Datapoints depict the mean phenotypic values of individual accessions, and the reaction norms represent the plastic response in the leaf area of each accession in response to drought. **F** Phenotypic reaction norms illustrating plastic and homeostatic responses in leaf area potential (t-test; *P*-value > 0.05). Violin distributions represent probability densities of leaf area potential among the accessions included in this study. Datapoints depict the leaf area potential of individual accessions, and the reaction norms represent the plastic response in the leaf area of leaf area potential of each accession in response to drought.

Figure 2. *SMALL AUXIN UP RNA 26* (*SAUR26*, AT3G03850) is a candidate regulator of leaf plasticity in response to drought. A. Manhattan plot representing the strength of association between genetic variants and leaf area plasticity in response to drought and illustration of the GO analysis enrichment found for the 50 variants displaying the strongest strength of association with this plasticity index. **B.** *SAUR26* gene model, including the two co-varying SNPs highlighted in **3B**. Orange block depicts the single exon, green block the 5' UTR, dark green the 3' UTR. Labels above indicate the position of the two SNPs that co-vary forming a haplotype in our sample. The illustration includes information on the major/minor allele corresponding to each of the SNPs, its frequency in our sample, in 189 accessions from the Iberian within the 1001 Genome Project, and in the whole 1001 Genome Project sample dataset. **C.** Manhattan plot representing the genome-wide strength of association between the genetic variation present within the 665 accessions from the transcript abundance reference panel used in this study (Kawakatsu et al., 2016) that overlap with the collection of accessions included in the 1001 Genomes project, and the variation in the transcript abundance of *SAUR26* (Kawakatsu et al., 2016). The peak in chromosome 3 represents the cis-genetic variants in *SAUR26* affecting its transcript abundance. For **B** and **C**, the score (y-axis) consists of the negative logarithm of the *P*-value and provides association strength. Each data point represents an SNP with a color corresponding to the chromosome where the genetic variants are located. The x-axis and the different colors shown in the SNPs depicted in the Manhattan plots represent the different chromosomes. The higher the score, the lower the P-value, and the stronger the association between genetic variation and leaf area plasticity or *SAUR26* transcript abundance. **D.** The minor haplotype of *SAUR26* is associated with negative plastic responses of leaf area potential in response to drought. Conversely, the major haplotype is associated with homeostatic or positive responses in leaf area potential in response to drought. Violin plots showing significantly different probability densities of leaf area plasticity in response to drought for the major and minor allele haplotypes in *SAUR26*. **E.** The haplotype in *SAUR26* associated with leaf area plasticity/homeostasis in response to drought is a regulatory haplotype. Violin plots showing significantly different probability densities of *SAUR26* transcript abundance for the major and minor allele haplotypes in *SAUR26* for both our sample and the entire Iberian population. **F.** Scatter

plot illustrating the positive relationship between leaf area plasticity index (y-axis) and *SAUR26* transcript abundance (x-axis). Grey shadow represents the 95% CI of the fit regression line (dark grey). **G**. Cartoon illustrating the regulatory role of genetic and transcript variation in *SAUR26* and the response of leaf area to drought.

Figure 3. Transcriptomic reaction norms uncover the genetic correlates of leaf area homeostasis in response to drought. A. Transcriptomic homeostatic reaction norms for leaf area in response to drought. This plot depicts the homeostatic relationship between the association of transcript abundance for each gene and leaf area potential under well-watered vs. drought conditions. Spearman's rank correlation coefficient ($r_{s;}$ y-axis) indicates the correlation between the leaf area potential and the natural variation in transcript abundance of each gene. The upper panel shows homeostatic reaction norms for transcripts significantly and positively correlated with leaf area potential under both watering regimes. The bottom panel shows homeostatic reaction norms for transcripts significantly and negatively correlated with leaf area potential under both watering regimes. **B** and **C**. Scatter plots depicting the relationship (*P*-value < 0.05) between leaf area potential under both well-watered and drought conditions (y-axis), and transcript abundance (FPKM; x-axis) of *ILI1 binding bHLH 1* (*IBH1,* AT2G43060) (**B)** and *RING-H2 GROUP F1A* (*RHF1A*; *AT4G14220*) **(C)**. In both (C) and (D), data were fitted using a linear regression model. Dark circles depict the leaf area potential of accessions grown under well-watered conditions, while gray squares depict the leaf area potential of accessions grown under drought.

Figure 4. Accessions with lower leaf area potential display leaf area homeostasis and higher water use efficiency as defined by $\delta^{13}C$. A. Negative relationship (*P*-value < 0.05) between leaf area plasticity in response to drought (y-axis) and leaf area potential under well-watered conditions (x-axis). Data were fitted using a linear regression model. Grey shadow represents the 95% CI of the fit regression line. Four different quadrants are defined by two dashed lines: the average leaf area potential (x-axis), and y = 0, which is the homeostatic point at which a change in water availability does not affect phenotypic potential. Data points depict individual accessions with their respective label. Data points are colored based on in which quadrant they fall (see text). **B**. The genetic basis of leaf area potential and plasticity in response to drought. Relationship between the GWAS associations found for the plastic responses in leaf area after drought (x-axis) (Table G3) and leaf area potential in the absence of drought (y-axis) (Table G1). Data points represent individual SNPs. Dashed lines depict an arbitrary threshold of 4 for significance. **C.** Transcriptomic association with leaf area potential under well-watered conditions and plastic leaf area responses to drought. Spearman's rank correlation depicts the relationship between the association for the transcript abundance of each gene in the Arabidopsis genome with leaf area plasticity in response to drought (r_s) in the y-axis and leaf area potential in the x-axis. Dashed lines define an arbitrary threshold to consider transcripts correlated positively ($r_s \geq 0.4$) or negatively ($r_s \leq -0.4$) with leaf area plasticity (y-axis) or net primary productivity (x-axis). **D.** Scatter plot illustrating the positive relationship (*P*-value < 0.05) between leaf area homeostasis in response to drought (leaf area

plasticity index, y-axis) and water use efficiency (x-axis) among Iberian Arabidopsis accessions used in this study. Data were fitted to a linear regression model. Grey shadow represents the 95% CI of the fit regression line (black). $\delta^{13}C$ data for the accessions studied here were retrieved from (Dittberner et al., 2018). As in panel **A**, four different quadrants are defined by two dashed lines: y = 0, which is the homeostatic point at which a change in water availability does not affect leaf area potential (i.e., a plasticity index of 0), and the average intrinsic water use efficiency (WUE_i, $\delta^{13}C$; x-axis). Data points depict individual accessions with their respective labels. **E.** The genetic basis of leaf area plasticity in response to drought and water use efficiency. This plot depicts the respective relationship between the GWAS associations found for the leaf area plasticity index in response to drought (y-axis) and water use efficiency (Dittberner et al., 2018) (x-axis). Data points represent individual SNPs. The y-axis and x-axis depict the extent of the association with, respectively, leaf area plasticity, and WUE_i, as the negative logarithm of the p-value. Dashed lines depict an arbitrary threshold for significance that is consistent across comparisons. **F.** Transcriptomic association with plastic leaf area responses to drought and WUE_i. Spearman's rank correlation depicts the relationship between the association for the transcript abundance of each gene in the Arabidopsis genome with leaf area plasticity in response to drought (r_s) in the y-axis and with WUE_i in the x-axis. Dashed lines define an arbitrary threshold to consider transcripts correlated positively ($r_s \geq 0.4$) or negatively ($r_s \leq -0.4$) with leaf area plasticity (y-axis) or net primary productivity (x-axis).

Figure 5. *CNGC16* and *AHA4* exemplify transcripts with opposing relationships to leaf area plasticity and water use efficiency. A and **B**. Scatter plots depicting the relationship (*P*-value < 0.05) between (**A**) leaf area plasticity index in response to drought or (**B**) water use efficiency (Dittberner et al., 2018) in the y-axis, and transcript abundance (FPKM) of *CYCLIC NUCLEOTIDE-GATED CHANNEL 16* (*CNGC16*) in the x-axis. **C** and **D**. Scatter plots depicting the relationship (P-value < 0.05) between leaf area plasticity index in response to drought (**5C**), or water use efficiency (**5D**) in the y-axis, and transcript abundance (FPKM) of *H^+-ATPase 4* (*AHA4*) in the x-axis. In all panels, data were fitted using a linear regression model. Grey shadow represents the 95% CI of the fit regression line.

Figure 6. Photosynthesis-related transcript variants regulate water use efficiency in Iberian Arabidopsis accessions. A. Manhattan plot representing the genome-wide strength of association between genetic variation and natural variation in $\delta^{13}C$ present within the 95 Iberian accessions of our study, with $\delta^{13}C$ values retrieved from (Dittberner et al., 2018). The score (y-axis) consists of the negative logarithm of the *P*-value and provides association strength. **Inset:** Violin plots representing the probability densities of water use efficiency for the major and minor allele haplotypes in *ClpX* for the accessions included in 6A**. B.** T-Manhattan plot representing transcriptome-wide strength of association between variation in transcript abundance (Kawakatsu et al., 2016) and natural variation in $\delta^{13}C$. In this analysis, we included the Iberian accessions with both transcript abundance data (Kawakatsu et al., 2016) and $\delta^{13}C$ information (Dittberner et al., 2018). The relationship is defined by the Spearman's rank correlation coefficient (r_s). Dashed lines define an arbitrary threshold for positive ($r_s \geq 0.4$) or negative ($r_s \leq -0.4$) correlation with water-use

efficiency (y-axis). **C**. Scatter plot depicting the positive relationship (*P*-value < 0.05) between WUE_i (y-axis) and *PLASMA MEMBRANE INTRINSIC PROTEIN 1;5* (*PIP1;5, AT4G23400*) transcript abundance for the Iberian accessions included in 6B. **D**. Scatter plot depicting the positive relationship (*P*-value < 0.05) between WUE_i (y-axis) and *RuBisCO SMALL SUBUNIT 2B* (*AT5G38420*; *RBCS2B*) transcript abundance for the Iberian accessions included in 6B. **E**. Scatter plot depicting the positive relationship (*P*-value < 0.05) between intrinsic water-use efficiency (WUE_i; y-axis) and *SMALL AUXIN UP RNA 26* (*SAUR26*, AT3G03850) transcript abundance for the Iberian accessions included in 6B. For **C**, **D**, and **E**, gray shadow represents the 95% CI of the fit regression line (black).

Acknowledgements

This research was supported by funding from The Pennsylvania State University to S.M.A.

References

Abudayyeh OO, Gootenberg JS, Essletzbichler P, Han S, Joung J, Belanto JJ, Verdine V, Cox DBT, Kellner MJ, Regev A, et al (2017) RNA targeting with CRISPR-Cas13. Nature 550: 280–284

Altman N, Krzywinski M (2016) Analyzing outliers: influential or nuisance? Nat Methods 13: 281–282

Angert AL, Huxman TE, Chesson P, Venable DL (2009) Functional tradeoffs determine species coexistence via the storage effect. Proc Natl Acad Sci USA 106: 11641–11645

Baek D, Kim MC, Kumar D, Park B, Cheong MS, Choi W, Park HC, Chun HJ, Park HJ, Lee SY, et al (2019) *AtPR5K2*, a *PR5-Like Receptor Kinase*, Modulates Plant Responses to drought Stress by *phosphorylating protein phosphatase 2Cs*. Front Plant Sci 10: 1146

Barton N, Hermisson J, Nordborg M (2019) Population genetics: Why structure matters. Elife 8: e45380

Billings WD, Mooney HA (1968) The ecology of arctic and alpine plants. Biol Rev 43: 481–529

Bouslama M, Schapaugh WT (1984) Stress tolerance in soybeans. I. evaluation of three screening techniques for heat and drought tolerance. Crop Sci 24: 933–937

Bradshaw AD (1965) Evolutionary significance of phenotypic plasticity in plants. Elsevier, pp 115–155

Cao J, Schneeberger K, Ossowski S, Günther T, Bender S, Fitz J, Koenig D, Lanz C, Stegle O, Lippert C, et al (2011) Whole-genome sequencing of multiple *Arabidopsis thaliana* populations. Nat Genet 43: 956–963

Chapin, FS (1991) Integrated responses of plants to stress. Bioscience 41: 29–36

Chen I-C, Hill JK, Ohlemüller R, Roy DB, Thomas CD (2011) Rapid range shifts of species

associated with high levels of climate warming. Science 333: 1024–1026

Cingolani P, Platts A, Wang LL, Coon M, Nguyen T, Wang L, Land SJ, Lu X, Ruden DM (2012) A program for annotating and predicting the effects of single nucleotide polymorphisms, SnpEff: SNPs in the genome of *Drosophila melanogaster* strain w1118; iso-2; iso-3. Fly (Austin) 6: 80–92

Coll JR, Aguilar E, Ashcroft L (2016) Drought variability and change across the Iberian Peninsula. Theoretical and Applied Climatology 1–16

Condon AG, Richards RA, Rebetzke GJ, Farquhar GD (2002) Improving intrinsic water-use efficiency and crop yield. Crop Sci 42: 122–131

Cook RD (1984) Assessment of local influence. doi: 10.21236/ADA143002

De Veylder L, Beeckman T, Beemster GT, Krols L, Terras F, Landrieu I, van der Schueren E, Maes S, Naudts M, Inzé D (2001) Functional analysis of cyclin-dependent kinase inhibitors of Arabidopsis. Plant Cell 13: 1653–1668

DeFalco TA, Moeder W, Yoshioka K (2016) Opening the gates: insights into cyclic nucleotide-gated channel-mediated signaling. Trends Plant Sci 21: 903–906

Des Marais DL, McKay JK, Richards JH, Sen S, Wayne T, Juenger TE (2012) Physiological genomics of response to soil drying in diverse Arabidopsis accessions. Plant Cell 24: 893–914

Dittberner H, Korte A, Mettler-Altmann T, Weber APM, Monroe G, de Meaux J (2018) Natural variation in stomata size contributes to the local adaptation of water-use efficiency in *Arabidopsis thaliana*. Mol Ecol 27: 4052–4065

Donat MG, Lowry AL, Alexander LV, O'Gorman PA, Maher N (2016) More extreme precipitation in the world's dry and wet regions. Nat Clim Chang 6: 508–513

Dorn LA, Pyle EH, Schmitt J (2000) Plasticity to light cues and resources in *Arabidopsis thaliana*: testing for adaptive value and costs. Evolution 54: 1982–1994

Du S-S, Li L, Li L, Wei X, Xu F, Xu P, Wang W, Xu P, Cao X, Miao L, et al (2020) Photoexcited *Cryptochrome2* interacts directly with *TOE1* and *TOE2* in flowering regulation. Plant Physiol 184: 487–505

Durvasula A, Fulgione A, Gutaker RM, Alacakaptan SI, Flood PJ, Neto C, Tsuchimatsu T, Burbano HA, Picó FX, Alonso-Blanco C, et al (2017) African genomes illuminate the early history and transition to selfing in *Arabidopsis thaliana*. Proc Natl Acad Sci USA 114: 5213–5218

Easlon HM, Nemali KS, Richards JH, Hanson DT, Juenger TE, McKay JK (2014) The physiological basis for genetic variation in water use efficiency and carbon isotope composition in *Arabidopsis thaliana*. Photosyn Res 119: 119–129

Easterling DR, Meehl GA, Parmesan C, Changnon SA, Karl TR, Mearns LO (2000) Climate extremes: observations, modeling, and impacts. Science 289: 2068–2074

Exposito-Alonso M, 500 Genomes Field Experiment Team, Burbano HA, Bossdorf O, Nielsen R, Weigel D (2019) Natural selection on the *Arabidopsis thaliana* genome in present and future climates. Nature 573: 126–129

Exposito-Alonso M, Brennan AC, Alonso-Blanco C, Picó FX (2018a) Spatio-temporal variation in

fitness responses to contrasting environments in *Arabidopsis thaliana*. Evolution. doi: 10.1111/evo.13508

Exposito-Alonso M, Vasseur F, Ding W, Wang G, Burbano HA, Weigel D (2018b) Genomic basis and evolutionary potential for extreme drought adaptation in *Arabidopsis thaliana*. Nat Ecol Evol 2: 352–358

Ferguson JN, Fernandes SB, Monier B, Miller ND, Allan D, Dmitrieva A, Schmuker P, Lozano R, Valluru R, Buckler ES, et al (2020) Machine learning enabled phenotyping for GWAS and TWAS of WUE traits in 869 field-grown sorghum accessions. BioRxiv. doi: 10.1101/2020.11.02.365213

Ferrero-Serrano Á, Assmann SM (2019) Phenotypic and genome-wide association with the local environment of Arabidopsis. Nat Ecol Evol 3: 274–285

Ferrero-Serrano Á, Assmann SM (2016) The α-subunit of the rice heterotrimeric G protein, RGA1, regulates drought tolerance during the vegetative phase in the dwarf rice mutant *d1*. J Exp Bot 67: 3433–3443

Ferrero-Serrano Á, Su Z, Assmann SM (2018) Illuminating the role of the Gα heterotrimeric G protein subunit, *RGA1*, in regulating photoprotection and photoavoidance in rice. Plant Cell Environ 41: 451–468

Fisher RA (1919) The correlation between relatives on the supposition of mendelian inheritance. Trans R Soc Edinb 52: 399–433

Forsman A (2015) Rethinking phenotypic plasticity and its consequences for individuals, populations and species. Heredity 115: 276–284

Frachon L, Bartoli C, Carrère S, Bouchez O, Chaubet A, Gautier M, Roby D, Roux F (2018) A genomic map of climate adaptation in *Arabidopsis thaliana* at a micro-geographic scale. Front Plant Sci 9: 967

Frachon L, Mayjonade B, Bartoli C, Hautekèete N-C, Roux F (2019) Adaptation to plant communities across the genome of *Arabidopsis thaliana*. Mol Biol Evol 36: 1442–1456

Galton F (1894) Natural inheritance. Macmillan and Company

Gao Q-M, Venugopal S, Navarre D, Kachroo A (2011) Low oleic acid-derived repression of jasmonic acid-inducible defense responses requires the *WRKY50* and *WRKY51* proteins. Plant Physiol 155: 464–476

Ge SX, Jung D, Yao R (2020) ShinyGO: a graphical gene-set enrichment tool for animals and plants. Bioinformatics 36: 2628–2629

Ghalambor CK, McKAY JK, Carroll SP, Reznick DN (2007) Adaptive versus non-adaptive phenotypic plasticity and the potential for contemporary adaptation in new environments. Funct Ecol 21: 394–407

Gomaa NH, Montesinos-Navarro A, Alonso-Blanco C, Picó FX (2011) Temporal variation in genetic diversity and effective population size of Mediterranean and subalpine *Arabidopsis thaliana* populations. Mol Ecol 20: 3540–3554

Grime JP (1977) Evidence for the existence of three primary strategies in plants and its relevance to ecological and evolutionary theory. Am Nat 111: 1169–1194

Groszmann M, Osborn HL, Evans JR (2017) Carbon dioxide and water transport through plant aquaporins. Plant Cell Environ 40: 938–961

Gusev A, Ko A, Shi H, Bhatia G, Chung W, Penninx BWJH, Jansen R, de Geus EJC, Boomsma DI, Wright FA, et al (2016) Integrative approaches for large-scale transcriptome-wide association studies. Nat Genet 48: 245–252

Hager A (2003) Role of the plasma membrane H+-ATPase in auxin-induced elongation growth: historical and new aspects. J Plant Res 116: 483–505

Haldrup A, Naver H, Scheller HV (1999) The interaction between plastocyanin and photosystem I is inefficient in transgenic Arabidopsis plants lacking the *PSI-N* subunit of photosystem I. Plant J 17: 689–698

Harrell Jr F, Dupont C (2019) Package 'Hmisc'. CRAN2018 2019: 235–6

Heinsch FA, Reeves M, Votava P, Kang S, Milesi C, Zhao M, Glassy J, Jolly WM, Loehman R, Bowker CF, et al (2003) Gpp and npp (mod17a2/a3) products nasa modis land algorithm. MOD17 User's Guide 1–57

Holt RD (1990) The microevolutionary consequences of climate change. Trends Ecol Evol (Amst) 5: 311–315

Ifuku K, Endo T, Shikanai T, Aro E-M (2011) Structure of the chloroplast NADH dehydrogenase-like complex: nomenclature for nuclear-encoded subunits. Plant Cell Physiol 52: 1560–1568

Ikeda M, Fujiwara S, Mitsuda N, Ohme-Takagi M (2012) A triantagonistic basic helix-loop-helix system regulates cell elongation in Arabidopsis. Plant Cell 24: 4483–4497

Johnson X, Wostrikoff K, Finazzi G, Kuras R, Schwarz C, Bujaldon S, Nickelsen J, Stern DB, Wollman F-A, Vallon O (2010) *MRL1*, a conserved Pentatricopeptide repeat protein, is required for stabilization of *rbcL* mRNA in Chlamydomonas and Arabidopsis. Plant Cell 22: 234–248

Juenger TE, McKay JK, Simms EI, Richards JH (2005) Identification and characterization of QTL underlying whole-plant physiology in *Arabidopsis thaliana*: $\delta^{13}C$, stomatal conductance and transpiration efficiency. Plant Cell Environ 28: 697–708

Kasuga M, Liu Q, Miura S, Yamaguchi-Shinozaki K, Shinozaki K (1999) Improving plant drought, salt, and freezing tolerance by gene transfer of a single stress-inducible transcription factor. Nat Biotechnol 17: 287–291

Kawakatsu T, Huang S-SC, Jupe F, Sasaki E, Schmitz RJ, Urich MA, Castanon R, Nery JR, Barragan C, He Y, et al (2016) Epigenomic diversity in a global collection of *Arabidopsis thaliana* accessions. Cell 166: 492–505

Kim J, Rudella A, Ramirez Rodriguez V, Zybailov B, Olinares PDB, van Wijk KJ (2009) Subunits of the plastid ClpPR protease complex have differential contributions to embryogenesis, plastid biogenesis, and plant development in Arabidopsis. Plant Cell 21: 1669–1692

Kimball S, Gremer JR, Angert AL, Huxman TE, Venable DL (2012) Fitness and physiology in a variable environment. Oecologia 169: 319–329

van Kleunen M, Fischer M (2005) Constraints on the evolution of adaptive phenotypic plasticity in plants. New Phytol 166: 49–60

Köhler C, Merkle T, Neuhaus G (1999) Characterisation of a novel gene family of putative cyclic nucleotide- and calmodulin-regulated ion channels in *Arabidopsis thaliana*. Plant J 18: 97–104

Korte A, Farlow A (2013) The advantages and limitations of trait analysis with GWAS: a review. Plant Methods 9: 29

Kremling KAG, Diepenbrock CH, Gore MA, Buckler ES, Bandillo NB (2019) Transcriptome-wide association supplements genome-wide association in *Zea mays*. G3 (Bethesda) 9: 3023–3033

Lan Y, Sun R, Ouyang J, Ding W, Kim M-J, Wu J, Li Y, Shi T (2021) AtMAD: *Arabidopsis thaliana* multi-omics association database. Nucleic Acids Res 49: D1445–D1451

Lasky JR, Des Marais DL, Lowry DB, Povolotskaya I, McKay JK, Richards JH, Keitt TH, Juenger TE (2014) Natural variation in abiotic stress responsive gene expression and local adaptation to climate in *Arabidopsis thaliana*. Mol Biol Evol 31: 2283–2296

Lefebvre S, Lawson T, Zakhleniuk OV, Lloyd JC, Raines CA, Fryer M (2005) Increased sedoheptulose-1,7-bisphosphatase activity in transgenic tobacco plants stimulates photosynthesis and growth from an early stage in development. Plant Physiol 138: 451–460

Leyser HM, Pickett FB, Dharmasiri S, Estelle M (1996) Mutations in the *AXR3* gene of Arabidopsis result in altered auxin response including ectopic expression from the *SAUR-AC1* promoter. Plant J 10: 403–413

Li Z-G, Chen H-W, Li Q-T, Tao J-J, Bian X-H, Ma B, Zhang W-K, Chen S-Y, Zhang J-S (2015) Three SAUR proteins *SAUR76*, *SAUR77* and *SAUR78* promote plant growth in Arabidopsis. Sci Rep 5: 12477

Liu J, Zhang Y, Qin G, Tsuge T, Sakaguchi N, Luo G, Sun K, Shi D, Aki S, Zheng N, et al (2008) Targeted degradation of the cyclin-dependent kinase inhibitor ICK4/KRP6 by RING-type E3 ligases is essential for mitotic cell cycle progression during Arabidopsis gametogenesis. Plant Cell 20: 1538–1554

Livingston AK, Cruz JA, Kohzuma K, Dhingra A, Kramer DM (2010) An Arabidopsis mutant with high cyclic electron flow around photosystem I (hcef) involving the NADPH dehydrogenase complex. Plant Cell 22: 221–233

Lobo JM, Castro I, Moreno JC (2001) Spatial and environmental determinants of vascular plant species richness distribution in the Iberian Peninsula and Balearic Islands. Biological Journal of the Linnean Society 73: 233–253

Loik ME, Breshears DD, Lauenroth WK, Belnap J (2004) A multi-scale perspective of water pulses in dryland ecosystems: climatology and ecohydrology of the western USA. Oecologia 141: 269–281

Maiwald D, Dietzmann A, Jahns P, Pesaresi P, Joliot P, Joliot A, Levin JZ, Salamini F, Leister D (2003) Knock-out of the genes coding for the Rieske protein and the ATP-synthase delta-subunit of Arabidopsis. Effects on photosynthesis, thylakoid protein composition, and nuclear chloroplast gene expression. Plant Physiol 133: 191–202

Manzano-Piedras E, Marcer A, Alonso-Blanco C, Picó FX (2014) Deciphering the adjustment

between environment and life history in annuals: lessons from a geographically-explicit approach in *Arabidopsis thaliana*. PLoS One 9: e87836

Marcer A, Vidigal DS, James PMA, Fortin MJ, Méndez-Vigo B, Hilhorst HWM, Bentsink L, Alonso-Blanco C, Picó FX (2018) Temperature fine-tunes Mediterranean *Arabidopsis thaliana* life-cycle phenology geographically. Plant Biol (Stuttg) 20 Suppl 1: 148–156

Meehl GA, Tebaldi C (2004) More intense, more frequent, and longer lasting heat waves in the 21st century. Science 305: 994–997

Méndez-Vigo B, Picó FX, Ramiro M, Martínez-Zapater JM, Alonso-Blanco C (2011) Altitudinal and climatic adaptation is mediated by flowering traits and FRI, FLC, and PHYC genes in Arabidopsis. Plant Physiol 157: 1942–1955

Montesinos A, Tonsor SJ, Alonso-Blanco C, Picó FX (2009) Demographic and genetic patterns of variation among populations of *Arabidopsis thaliana* from contrasting native environments. PLoS One 4: e7213

Montesinos-Navarro A, Wig J, Pico FX, Tonsor SJ (2011) *Arabidopsis thaliana* populations show clinal variation in a climatic gradient associated with altitude. New Phytol 189: 282–294

Moreno JE, Moreno-Piovano G, Chan RL (2018) The antagonistic basic helix-loop-helix partners BEE and IBH1 contribute to control plant tolerance to abiotic stress. Plant Sci 271: 143–150

Murakami R, Ifuku K, Takabayashi A, Shikanai T, Endo T, Sato F (2005) Functional dissection of two Arabidopsis PsbO proteins: *PsbO1* and *PsbO2*. FEBS J 272: 2165–2175

Nagatoshi Y, Ikeda M, Kishi H, Hiratsu K, Muraguchi A, Ohme-Takagi M (2016) Induction of a dwarf phenotype with IBH1 may enable increased production of plant-made pharmaceuticals in plant factory conditions. Plant Biotechnol J 14: 887–894

Niopek-Witz S, Deppe J, Lemieux MJ, Möhlmann T (2014) Biochemical characterization and structure-function relationship of two plant NCS2 proteins, the nucleobase transporters *NAT3* and *NAT12* from *Arabidopsis thaliana*. Biochim Biophys Acta 1838: 3025–3035

Nishimura K, van Wijk KJ (2015) Organization, function and substrates of the essential Clp protease system in plastids. Biochim Biophys Acta 1847: 915–930

Oh E, Zhu J-Y, Bai M-Y, Arenhart RA, Sun Y, Wang Z-Y (2014) Cell elongation is regulated through a central circuit of interacting transcription factors in the Arabidopsis hypocotyl. Elife. doi: 10.7554/eLife.03031

Ohashi-Ito K, Matsukawa M, Fukuda H (2013) An atypical bHLH transcription factor regulates early xylem development downstream of auxin. Plant Cell Physiol 54: 398–405

Parsons RF (1968) The significance of growth-rate comparisons for plant ecology. Am Nat 102: 595–597

Páscoa P, Gouveia CM, Russo A, Trigo RM (2017) Drought Trends in the Iberian Peninsula over the Last 112 Years. Advances in Meteorology 2017: 1–13

Picó FX (2012) Demographic fate of *Arabidopsis thaliana* cohorts of autumn- and spring-germinated plants along an altitudinal gradient. J Ecol 100: 1009–1018

Picó FX, Méndez-Vigo B, Martínez-Zapater JM, Alonso-Blanco C (2008) Natural genetic variation of *Arabidopsis thaliana* is geographically structured in the Iberian peninsula. Genetics 180:

1009–1021
Pols AJ, Spahn A (2014) Biofuels: ethical issues. Encyclopedia of Food and Agricultural Ethics 211–217
Price AL, Zaitlen NA, Reich D, Patterson N (2010) New approaches to population stratification in genome-wide association studies. Nat Rev Genet 11: 459–463
Rey Benayas JM, Scheiner SM (2002) Plant diversity, biogeography and environment in Iberia: Patterns and possible causal factors. J Veg Sci 13: 245
Richards CL, Bossdorf O, Muth NZ, Gurevitch J, Pigliucci M (2006) Jack of all trades, master of some? On the role of phenotypic plasticity in plant invasions. Ecol Lett 9: 981–993
Rober-Kleber N, Albrechtová JTP, Fleig S, Huck N, Michalke W, Wagner E, Speth V, Neuhaus G, Fischer-Iglesias C (2003) Plasma membrane H^+-ATPase is involved in auxin-mediated cell elongation during wheat embryo development. Plant Physiol 131: 1302–1312
Running SW, Zhao M (2015) Daily GPP and annual NPP (MOD17A2/A3) products NASA Earth Observing System MODIS land algorithm. MOD17 User's Guide 2015: 1–28
Salehin M, Li B, Tang M, Katz E, Song L, Ecker JR, Kliebenstein DJ, Estelle M (2019) Auxin-sensitive Aux/IAA proteins mediate drought tolerance in Arabidopsis by regulating glucosinolate levels. Nat Commun 10: 4021
Sasaki E, Köcher T, Filiault DL, Nordborg M (2021) Revisiting a GWAS peak in *Arabidopsis thaliana* reveals possible confounding by genetic heterogeneity. BioRxiv. doi: 10.1101/2021.02.03.429533
Schär C, Vidale PL, Lüthi D, Frei C, Häberli C, Liniger MA, Appenzeller C (2004) The role of increasing temperature variability in European summer heatwaves. Nature 427: 332–336
Schindele A, Dorn A, Puchta H (2020) CRISPR/Cas brings plant biology and breeding into the fast lane. Curr Opin Biotechnol 61: 7–14
Schweizer F, Fernández-Calvo P, Zander M, Diez-Diaz M, Fonseca S, Glauser G, Lewsey MG, Ecker JR, Solano R, Reymond P (2013) Arabidopsis basic helix-loop-helix transcription factors MYC2, MYC3, and MYC4 regulate glucosinolate biosynthesis, insect performance, and feeding behavior. Plant Cell 25: 3117–3132
Seren Ü, Vilhjálmsson BJ, Horton MW, Meng D, Forai P, Huang YS, Long Q, Segura V, Nordborg M (2012) GWAPP: a web application for genome-wide association mapping in Arabidopsis. Plant Cell 24: 4793–4805
Siepielski AM, Morrissey MB, Buoro M, Carlson SM, Caruso CM, Clegg SM, Coulson T, DiBattista J, Gotanda KM, Francis CD, et al (2017) Precipitation drives global variation in natural selection. Science 355: 959–962
Sohail M, Maier RM, Ganna A, Bloemendal A, Martin AR, Turchin MC, Chiang CW, Hirschhorn J, Daly MJ, Patterson N, et al (2019) Polygenic adaptation on height is overestimated due to uncorrected stratification in genome-wide association studies. Elife. doi: 10.7554/eLife.39702
Spartz AK, Ren H, Park MY, Grandt KN, Lee SH, Murphy AS, Sussman MR, Overvoorde PJ, Gray WM (2014) SAUR inhibition of PP2C-D Phosphatases activates plasma membrane H+-

ATPases to promote cell expansion in arabidopsis. Plant Cell 26: 2129–2142
Stortenbeker N, Bemer M (2019) The SAUR gene family: the plant's toolbox for adaptation of growth and development. J Exp Bot 70: 17–27
Tabas-Madrid D, Méndez-Vigo B, Arteaga N, Marcer A, Pascual-Montano A, Weigel D, Xavier Picó F, Alonso-Blanco C (2018) Genome-wide signatures of flowering adaptation to climate temperature: regional analyses in a highly diverse native range of *Arabidopsis thaliana*. Plant Cell Environ 41: 1806–1820
Takahashi K, Hayashi K, Kinoshita T (2012) Auxin activates the plasma membrane H+-ATPase by phosphorylation during hypocotyl elongation in Arabidopsis. Plant Physiol 159: 632–641
Team RC (2013) R: A language and environment for statistical computing.
The 1001 Genomes Consortium (2016) 1,135 Genomes reveal the global pattern of polymorphism in *Arabidopsis thaliana*. Cell 166: 481–491
Tilman D (1988) Plant strategies and the dynamics and structure of plant communities. Princeton University Press
Tunc-Ozdemir M, Tang C, Ishka MR, Brown E, Groves NR, Myers CT, Rato C, Poulsen LR, McDowell S, Miller G, et al (2013) A cyclic nucleotide-gated channel (CNGC16) in pollen is critical for stress tolerance in pollen reproductive development. Plant Physiol 161: 1010–1020
Varvel GE, Vogel KP, Mitchell RB, Follett RF, Kimble JM (2008) Comparison of corn and switchgrass on marginal soils for bioenergy. Biomass and Bioenergy 32: 18–21
Via S, Gomulkiewicz R, De Jong G, Scheiner SM, Schlichting CD, Van Tienderen PH (1995) Adaptive phenotypic plasticity: consensus and controversy. Trends Ecol Evol (Amst) 10: 212–217
Vicente-Serrano SM (2006a) Spatial and temporal analysis of droughts in the Iberian Peninsula (1910–2000). Hydrological Sciences Journal 51: 83–97
Vicente-Serrano SM (2006b) Differences in spatial patterns of drought on different time scales: an analysis of the iberian peninsula. Water Resour Manage 20: 37–60
Vidigal DS, Marques ACSS, Willems LAJ, Buijs G, Méndez-Vigo B, Hilhorst HWM, Bentsink L, Picó FX, Alonso-Blanco C (2016) Altitudinal and climatic associations of seed dormancy and flowering traits evidence adaptation of annual life cycle timing in *Arabidopsis thaliana*. Plant Cell Environ 39: 1737–1748
Waddington CH (1953) Genetic assimilation of an acquired character. Evolution 7: 118
Wang Y-F, Munemasa S, Nishimura N, Ren H-M, Robert N, Han M, Puzõrjova I, Kollist H, Lee S, Mori I, et al (2013) Identification of cyclic GMP-activated nonselective Ca2+-permeable cation channels and associated CNGC5 and CNGC6 genes in Arabidopsis guard cells. Plant Physiol 163: 578–590
Wang Z, Yang L, Liu Z, Lu M, Wang M, Sun Q, Lan Y, Shi T, Wu D, Hua J (2019) Natural variations of growth thermo-responsiveness determined by SAUR26/27/28 proteins in *Arabidopsis thaliana*. New Phytol 224: 291–305
Wang Z, Yang L, Wu D, Zhang N, Hua J (2021) Polymorphisms in cis-elements confer SAUR26

gene expression difference for thermo-response natural variation in Arabidopsis. New Phytol 229: 2751–2764

Waters BM, Chu H-H, Didonato RJ, Roberts LA, Eisley RB, Lahner B, Salt DE, Walker EL (2006) Mutations in Arabidopsis yellow stripe-like1 and yellow stripe-like3 reveal their roles in metal ion homeostasis and loading of metal ions in seeds. Plant Physiol 141: 1446–1458

West-Eberhard MJ (2003) Developmental plasticity and evolution. Oxford University Press

Wickham H, Francois R, Henry L, Müller K (2015) dplyr: A grammar of data manipulation. R package version 0.4 3:

Wickham H, Henry L (2018) tidyr: Easily Tidy Data with ‘spread ()’and ‘gather ()’Functions. R package version 0.8 2:

Wolfe MD, Tonsor SJ (2014) Adaptation to spring heat and drought in northeastern Spanish *Arabidopsis thaliana*. New Phytol 201: 323–334

Yamori W, Sakata N, Suzuki Y, Shikanai T, Makino A (2011) Cyclic electron flow around photosystem I via chloroplast NAD(P)H dehydrogenase (NDH) complex performs a significant physiological role during photosynthesis and plant growth at low temperature in rice. Plant J 68: 966–976

Zhang H, Zhao Y, Zhu J-K (2020) Thriving under stress: how plants balance growth and the stress response. Dev Cell 55: 529–543

Zhang J, Vankova R, Malbeck J, Dobrev PI, Xu Y, Chong K, Neff MM (2009) *AtSOFL1* and *AtSOFL2* act redundantly as positive modulators of the endogenous content of specific cytokinins in Arabidopsis. PLoS One 4: e8236

Zheng Q, Zheng Y, Ji H, Burnie W, Perry SE (2016) Gene regulation by the *AGL15* transcription factor reveals hormone interactions in somatic embryogenesis. Plant Physiol 172: 2374–2387

Zhiponova MK, Morohashi K, Vanhoutte I, Machemer-Noonan K, Revalska M, Van Montagu M, Grotewold E, Russinova E (2014) Helix-loop-helix/basic helix-loop-helix transcription factor network represses cell elongation in Arabidopsis through an apparent incoherent feed-forward loop. Proc Natl Acad Sci USA 111: 2824–2829

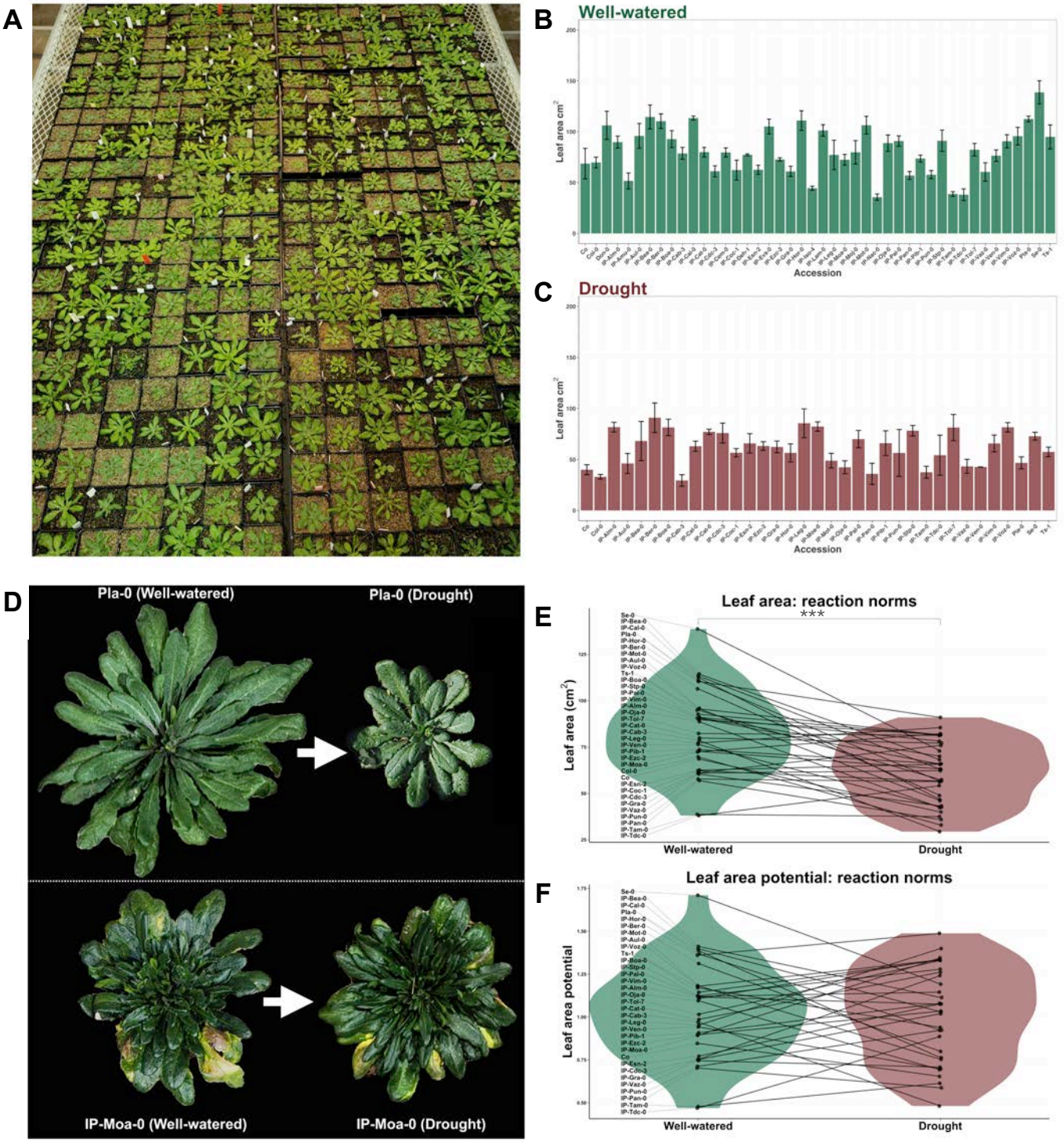

Figure 1. Rosette leaf area observations at the time of flowering used to calculate leaf area potential and plasticity in this study (Table S1). A. Detail of the common garden experiment, illustrating the randomization of well-watered and drought treatments, as reflected in soil coloration. **B.** Leaf areas for accessions grown under optimal conditions. **C**. Leaf areas for accessions under drought conditions. Accessions are arranged alphabetically. Bars represent means ±SE. **D.** Images illustrating the plastic and homeostatic responses to drought found among the accessions included in this study. **E.** Phenotypic reaction norms illustrating an overall reduction of leaf area in response to drought (t-test; P-value < 0.001). Violin distributions represent probability densities of leaf area (cm^2) among the accessions included in this study. Datapoints depict the mean phenotypic values of individual accessions, and the reaction norms represent the plastic response in the leaf area of each accession in response to drought. **F** Phenotypic reaction norms illustrating plastic and homeostatic responses in leaf area potential (t-test; P-value > 0.05). Violin distributions represent probability densities of leaf area potential among the accessions included in this study. Datapoints depict the leaf area potential of individual accessions, and the reaction norms represent the plastic response in the leaf area of leaf area potential of each accession in response to drought.

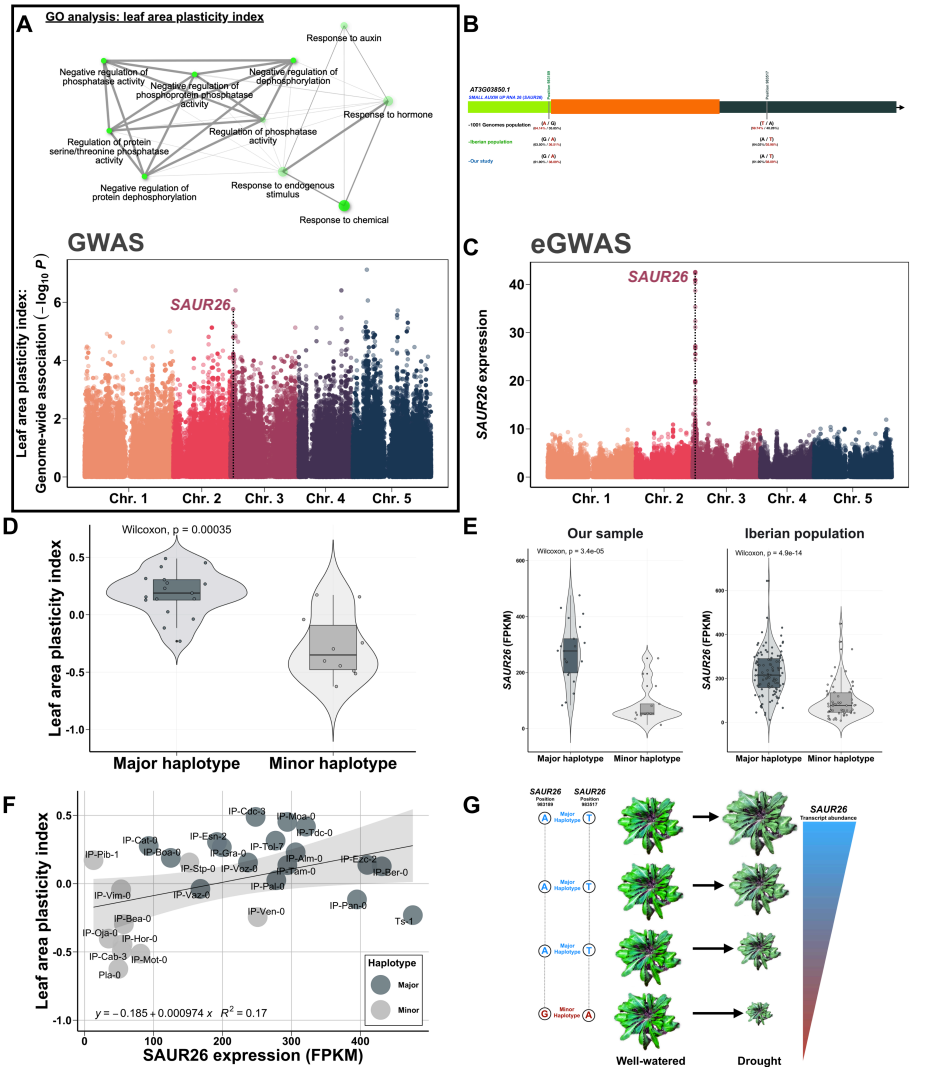

Figure 2. *SMALL AUXIN UP RNA 26* (*SAUR26*, AT3G03850) is a candidate regulator of leaf plasticity in response to drought. A. Manhattan plot representing the strength of association between genetic variants and leaf area plasticity in response to drought and illustration of the GO analysis enrichment found for the 50 variants displaying the strongest strength of association with this plasticity index. **B.** *SAUR26* gene model, including the two co-varying SNPs highlighted in **3B**. Orange block depicts the single exon, green block the 5' UTR, dark green the 3' UTR. Labels above indicate the position of the two SNPs that co-vary forming a haplotype in our sample. The illustration includes information on the major/minor allele corresponding to each of the SNPs, its frequency in our sample, in 189 accessions from the Iberian within the 1001 Genome Project, and in the whole 1001 Genome Project sample dataset. **C.** Manhattan plot representing the genome-wide strength of association between the genetic variation present within the 665 accessions from the transcript abundance reference panel used in this study (Kawakatsu et al., 2016) that overlap with the collection of accessions included in the 1001 Genomes project, and the variation in the transcript abundance of *SAUR26* (Kawakatsu et al., 2016). The peak in chromosome 3 represents the cis-genetic variants in *SAUR26* affecting its transcript abundance. For **B** and **C**, the score (y-axis) consists of the negative logarithm of the *P*-value and provides association strength. Each data point represents an SNP with a color corresponding to the chromosome where the genetic variants are located. The x-axis and the different colors shown in the SNPs depicted in the Manhattan plots represent the different chromosomes. The higher the score, the lower the P-value, and the stronger the association between genetic variation and leaf area plasticity or *SAUR26* transcript abundance. **D.** The minor haplotype of *SAUR26* is associated with negative plastic responses of leaf area potential in response to drought. Conversely, the major haplotype is associated with homeostatic or positive responses in leaf area potential in response to drought. Violin plots showing significantly different probability densities of leaf area plasticity in response to drought for the major and minor allele haplotypes in *SAUR26.* **E.** The haplotype in *SAUR26* associated with leaf area plasticity/homeostasis in response to drought is a regulatory haplotype. Violin plots showing significantly different probability densities of *SAUR26* transcript abundance for the major and minor allele haplotypes in *SAUR26* for both our sample and the entire Iberian population. **F.** Scatter plot illustrating the positive relationship between leaf area plasticity index (y-axis) and *SAUR26* transcript abundance (x-axis). Grey shadow represents the 95% CI of the fit regression line (dark grey). **G**. Cartoon illustrating the regulatory role of genetic and transcript variation in *SAUR26* and the response of leaf area to drought.

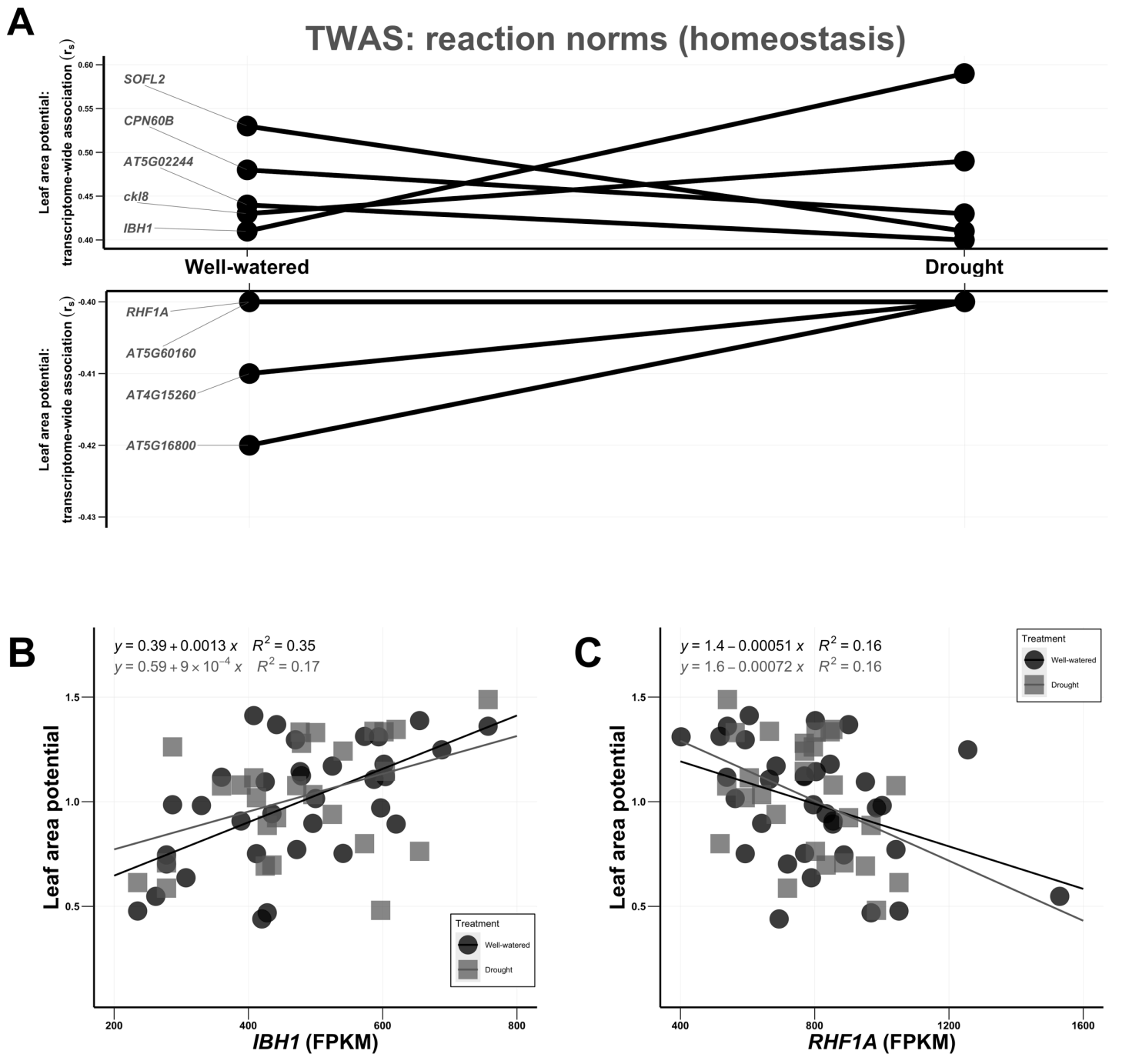

Figure 3. Transcriptomic reaction norms uncover the genetic correlates of leaf area homeostasis in response to drought. A. Transcriptomic homeostatic reaction norms for leaf area in response to drought. This plot depicts the homeostatic relationship between the association of transcript abundance for each gene and leaf area potential under well-watered vs. drought conditions. Spearman's rank correlation coefficient (r_s; y-axis) indicates the correlation between the leaf area potential and the natural variation in transcript abundance of each gene. The upper panel shows homeostatic reaction norms for transcripts significantly and positively correlated with leaf area potential under both watering regimes. The bottom panel shows homeostatic reaction norms for transcripts significantly and negatively correlated with leaf area potential under both watering regimes. **B** and **C**. Scatter plots depicting the relationship (P-value < 0.05) between leaf area potential under both well-watered and drought conditions (y-axis), and transcript abundance (FPKM; x-axis) of *ILI1 binding bHLH 1* **(***IBH1,* AT2G43060) **(B)** and *RING-H2 GROUP F1A* (*RHF1A*; *AT4G14220*) **(C)**. In both (C) and (D), data were fitted using a linear regression model. Dark circles depict the leaf area potential of accessions grown under well-watered conditions, while gray squares depict the leaf area potential of accessions grown under drought.

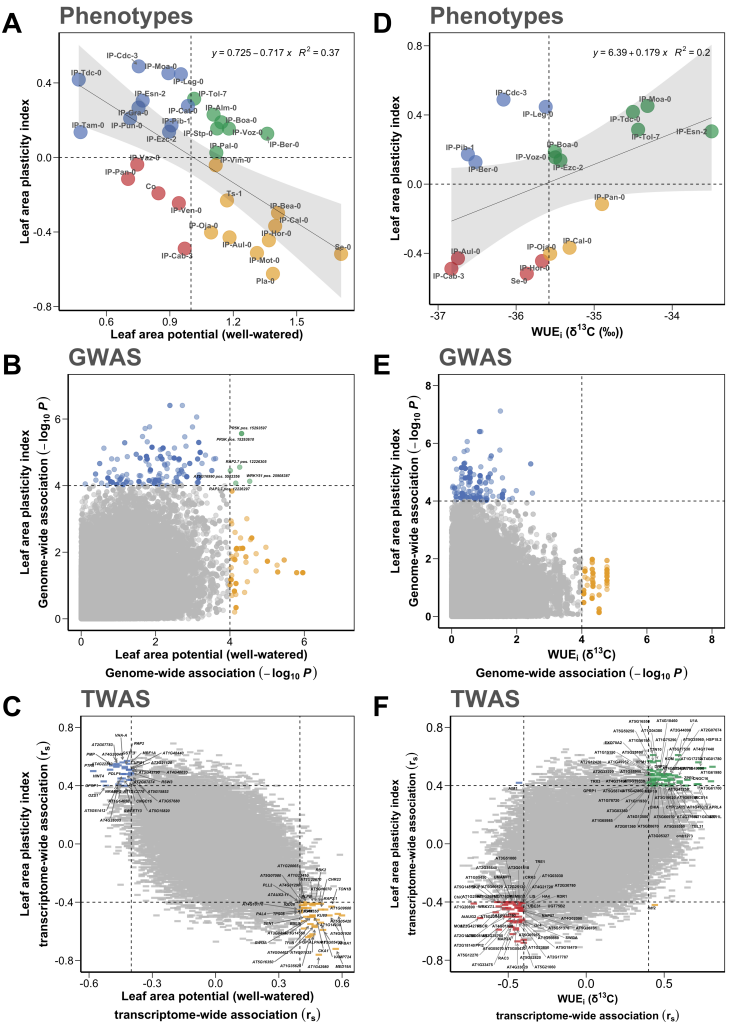

Figure 4. Accessions with lower leaf area potential display leaf area homeostasis and higher water use efficiency as defined by $\delta^{13}C$. A. Negative relationship (*P*-value < 0.05) between leaf area plasticity in response to drought (y-axis) and leaf area potential under well-watered conditions (x-axis). Data were fitted using a linear regression model. Grey shadow represents the 95% CI of the fit regression line. Four different quadrants are defined by two dashed lines: the average leaf area potential (x-axis), and y = 0, which is the homeostatic point at which a change in water availability does not affect phenotypic potential. Data points depict individual accessions with their respective label. Data points are colored based on in which quadrant they fall (see text). **B**. The genetic basis of leaf area potential and plasticity in response to drought. Relationship between the GWAS associations found for the plastic responses in leaf area after drought (x-axis) (Table G3) and leaf area potential in the absence of drought (y-axis) (Table G1). Data points represent individual SNPs. Dashed lines depict an arbitrary threshold of 4 for significance. **C.** Transcriptomic association with leaf area potential under well-watered conditions and plastic leaf area responses to drought. Spearman's rank correlation depicts the relationship between the association for the transcript abundance of each gene in the Arabidopsis genome with leaf area plasticity in response to drought (r_s) in the y-axis and leaf area potential in the x-axis. Dashed lines define an arbitrary threshold to consider transcripts correlated positively ($r_s \geq 0.4$) or negatively ($r_s \leq -0.4$) with leaf area plasticity (y-axis) or net primary productivity (x-axis). **D.** Scatter plot illustrating the positive relationship (*P*-value < 0.05) between leaf area homeostasis in response to drought (leaf area plasticity index, y-axis) and water use efficiency (x-axis) among Iberian Arabidopsis accessions used in this study. Data were fitted to a linear regression model. Grey shadow represents the 95% CI of the fit regression line (black). $\delta^{13}C$ data for the accessions studied here were retrieved from (Dittberner et al., 2018). As in panel **A**, four different quadrants are defined by two dashed lines: y = 0, which is the homeostatic point at which a change in water availability does not affect leaf area potential (i.e., a plasticity index of 0), and the average intrinsic water use efficiency (WUE_i, $\delta^{13}C$; x-axis). Data points depict individual accessions with their respective labels. **E.** The genetic basis of leaf area plasticity in response to drought and water use efficiency. This plot depicts the respective relationship between the GWAS associations found for the leaf area plasticity index in response to drought (y-axis) and water use efficiency (Dittberner et al., 2018) (x-axis). Data points represent individual SNPs. The y-axis and x-axis depict the extent of the association with, respectively, leaf area plasticity, and WUE_i, as the negative logarithm of the p-value. Dashed lines depict an arbitrary threshold for significance that is consistent across comparisons. **F.** Transcriptomic association with plastic leaf area responses to drought and WUE_i. Spearman's rank correlation depicts the relationship between the association for the transcript abundance of each gene in the Arabidopsis genome with leaf area plasticity in response to drought (r_s) in the y-axis and with WUE_i in the x-axis. Dashed lines define an arbitrary threshold to consider transcripts correlated positively ($r_s \geq 0.4$) or negatively ($r_s \leq -0.4$) with leaf area plasticity (y-axis) or net primary productivity (x-axis).

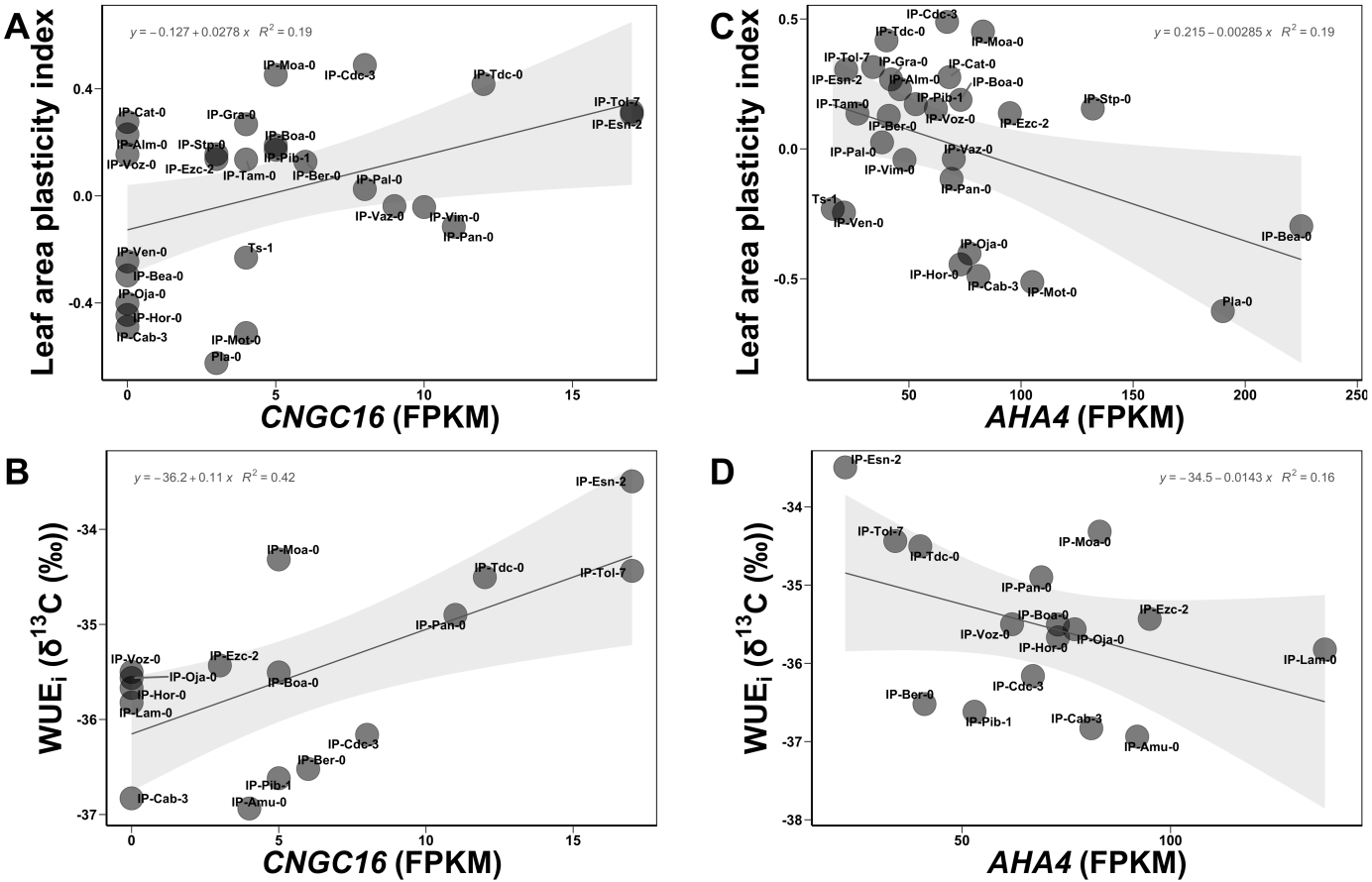

Figure 5. *CNGC16* and *AHA4* exemplify transcripts with opposing relationships to leaf area plasticity and water use efficiency. A and **B**. Scatter plots depicting the relationship (*P*-value < 0.05) between (**A**) leaf area plasticity index in response to drought or (**B**) water use efficiency (Dittberner et al., 2018) in the y-axis, and transcript abundance (FPKM) of *CYCLIC NUCLEOTIDE-GATED CHANNEL 16* (*CNGC16*) in the x-axis. **C** and **D**. Scatter plots depicting the relationship (P-value < 0.05) between leaf area plasticity index in response to drought (**5C**), or water use efficiency (**5D**) in the y-axis, and transcript abundance (FPKM) of *H^+-ATPase 4* (*AHA4*) in the x-axis. In all panels, data were fitted using a linear regression model. Grey shadow represents the 95% CI of the fit regression line.

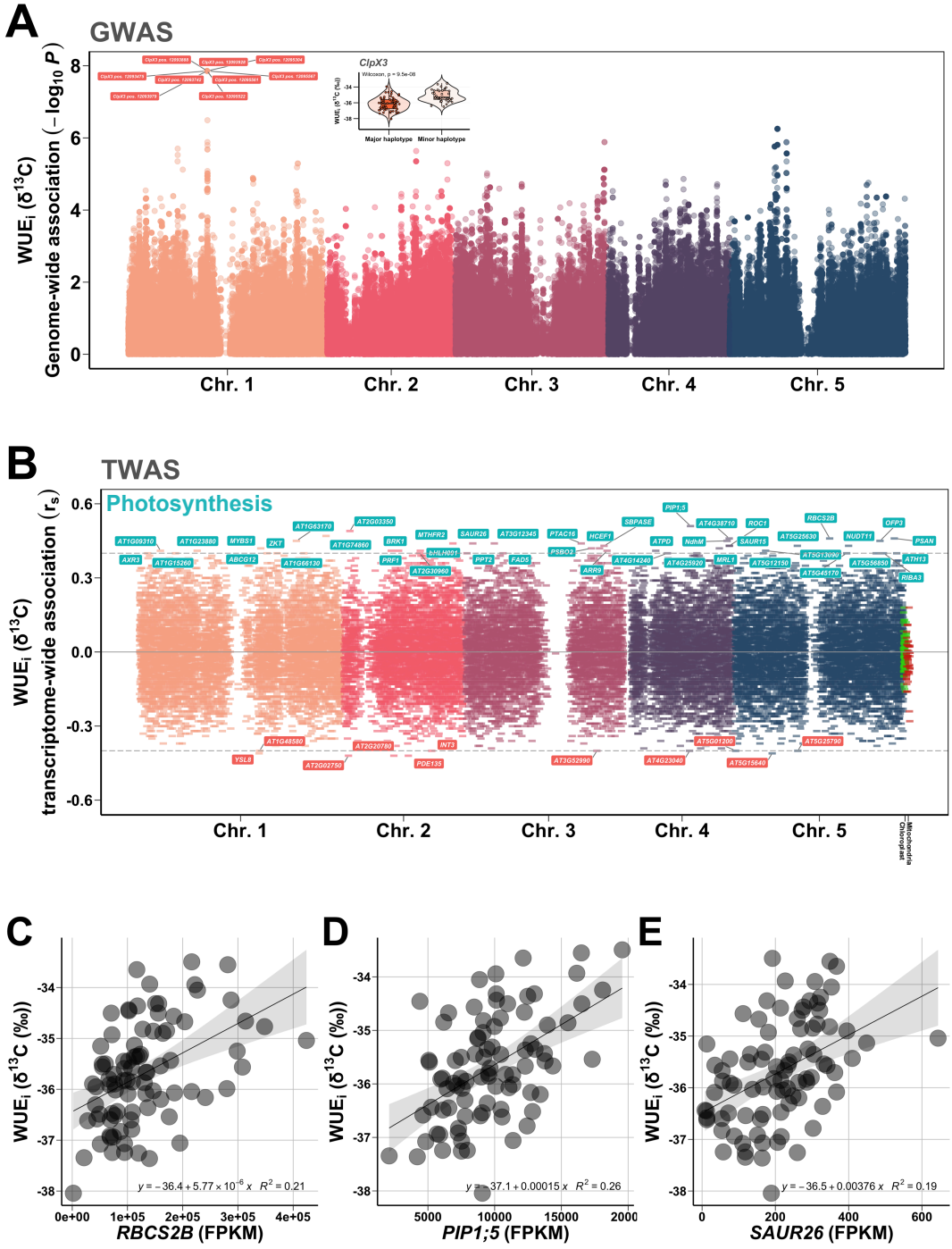

Figure 6. Photosynthesis-related transcript variants regulate water use efficiency in Iberian Arabidopsis accessions. A. Manhattan plot representing the genome-wide strength of association between genetic variation and natural variation in $\delta^{13}C$ present within the 95 Iberian accessions of our study, with $\delta^{13}C$ values retrieved from (Dittberner et al., 2018). The score (y-axis) consists of the negative logarithm of the *P*-value and provides association strength. Inset**:** Violin plots representing the probability densities of water use efficiency for the major and minor allele haplotypes in *ClpX* for the accessions included in 6A**. B.** T-Manhattan plot representing transcriptome-wide strength of association between variation in transcript abundance (Kawakatsu et al., 2016) and natural variation in $\delta^{13}C$. In this analysis, we included the Iberian accessions with both transcript abundance data (Kawakatsu et al., 2016) and $\delta^{13}C$ information (Dittberner et al., 2018). The relationship is defined by the Spearman's rank correlation coefficient (r_s). Dashed lines define an arbitrary threshold for positive ($r_s \geq 0.4$) or negative ($r_s \leq -0.4$) correlation with water-use efficiency (y-axis). **C**. Scatter plot depicting the positive relationship (*P*-value < 0.05) between WUE_i (y-axis) and *PLASMA MEMBRANE INTRINSIC PROTEIN 1;5* **(***PIP1;5, AT4G23400***)** transcript abundance for the Iberian accessions included in 6B. **D**. Scatter plot depicting the positive relationship (*P*-value < 0.05) between WUE_i (y-axis) and *RuBisCO SMALL SUBUNIT 2B* (*AT5G38420*; *RBCS2B*) transcript abundance for the Iberian accessions included in 6B. **E**. Scatter plot depicting the positive relationship (*P*-value < 0.05) between intrinsic water-use efficiency (WUE_i; y-axis) and *SMALL AUXIN UP RNA 26* (*SAUR26,* AT3G03850) transcript abundance for the Iberian accessions included in 6B. For **C**, **D**, and **E**, gray shadow represents the 95% CI of the fit regression line (black).